



**Citation:** Bartolucci, M., & Veneri, F. (2024). The phenological soil water balance: a proposed model for estimating water resources for an entire watershed using crop coefficients. *Italian Journal of Agrometeorology* (1): 17-48. doi: 10.36253/ijam-2334

**Received:** October 16, 2023

**Accepted:** June 8, 2024

**Published:** August 2, 2024

**Copyright:** ©2024 Bartolucci, M., & Veneri, F. This is an open access, peer-reviewed article published by Firenze University Press (<http://www.fupress.com/ijam>) and distributed under the terms of the Creative Commons Attribution License, which permits unrestricted use, distribution, and reproduction in any medium, provided the original author and source are credited.

**Data Availability Statement:** All relevant data are within the paper and its Supporting Information files.

**Competing Interests:** The Author(s) declare(s) no conflict of interest.

**ORCID:**

MB: 0000-0002-1972-2228

FV: 0000-0002-4881-1609

## The phenological soil water balance: a proposed model for estimating water resources for an entire watershed using crop coefficients

MICHELE BARTOLUCCI<sup>1,\*</sup>, FRANCESCO VENERI<sup>2</sup>

<sup>1</sup> *Independent researcher, Urbino, Italy*

<sup>2</sup> *Dipartimento di Scienze Pure e Applicate, Università degli Studi di Urbino Carlo Bo, Campus Scientifico "Enrico Mattei", via Ca' le Suore 2/4, 61029 - Urbino (PU), Italy*

\*Corresponding author. Email: [michele.bartolucci1@uniurb.it](mailto:michele.bartolucci1@uniurb.it)

**Abstract.** The aim of the research was to develop a model that would allow the application, at a watershed scale, of the hydrological soil water balance model proposed by the FAO for the dosing of irrigation water in agriculture, which uses crop coefficients ( $K_c$ ) for the calculation of potential crop evapotranspiration ( $ET_c$ ). To be able to assess the water resources of a territory in which there are land uses other than agricultural ones, the application of the proposed model has made it necessary to determine the crop coefficients of the latter. Since crop coefficients vary according to phenological stage, this model was termed 'phenological soil water balance'. A correction factor for precipitation and potential evapotranspiration, using an acclivity coefficient (i.e., the ratio between the actual area and the projected area), has also been proposed to obtain accurate results even in non-flat areas, which allowed us to consider the actual area of the territory instead of the projected one. The model was applied daily for 7 consecutive years (from 2013 to 2019) in the Santa Maria degli Angeli watershed (Urbino, central Italy) whose area is about 14 km<sup>2</sup>. The calibration and validation of the model were conducted by comparing the deep percolation computed by the model with baseflow values of the Santa Maria degli Angeli stream obtained by flow measurements made at the closing section of the sample watershed. The results of the model showed that the total values of deep percolation and measured baseflow only differed by 3% in the whole period considered; thus the phenological soil water balance model can be used to accurately estimate water resources and can be applied at different time intervals (daily, monthly, annual, etc.). The structure of the model makes it suitable for application in both small and large watersheds and territories.

**Keywords:** water resources management, watershed deficit, soil water balance, actual evapotranspiration, deep percolation.

### HIGHLIGHTS

- Water scarcity due to climate change makes it necessary to better manage water resources
- Water management requires the computation of the soil water balance of a territory

- This study implemented a daily soil water balance model based on phenological stages
- Soil water balance models generally consider crop coefficients only for agricultural lands
- This model proposes crop coefficients also for non-agricultural land use

1. INTRODUCTION

Human beings use freshwater for several purposes, for drinking and other domestic uses, irrigation, energy production, industrial processes, and so forth. Freshwater is a renewable resource but the increase in the global population, growing industrialisation, growing demand for water for irrigation, soil consumption, and the use of agrochemicals in agriculture pose serious threats to its availability and quality.

Climate change is another important factor that will influence the future availability of freshwater. For each degree Celsius of global warming, approximately 7% of the global population is projected to be exposed to

a decrease of renewable water resources of at least 20% (Jimenez et al., 2014). If global mean temperatures were to increase by 1°C from the 1990s, Schewe et al. (2013) estimated that about 8% of the global population would see a severe reduction in freshwater resources; this percentage would rise to 14% with a temperature increase of 2°C and to 17% with an increase of 3°C. For these reasons, proper management of water resources is indispensable to ensure water use sustainability and maintain environmental, social, and economic welfare, which must be preceded by an accurate estimation of the water resources themselves. This can be achieved through the calculation of the soil water balance using hydrological models capable of reproducing hydrological processes with a certain accuracy based on input parameters.

The inputs used by different models are representative of the geomorphological and microclimatic characteristics of the watershed. These are precipitation, air temperature, soil properties, topography, vegetation, hydrogeology, and other physical parameters. Models can be applied in very complex and large watersheds (Gayathri et al., 2015).

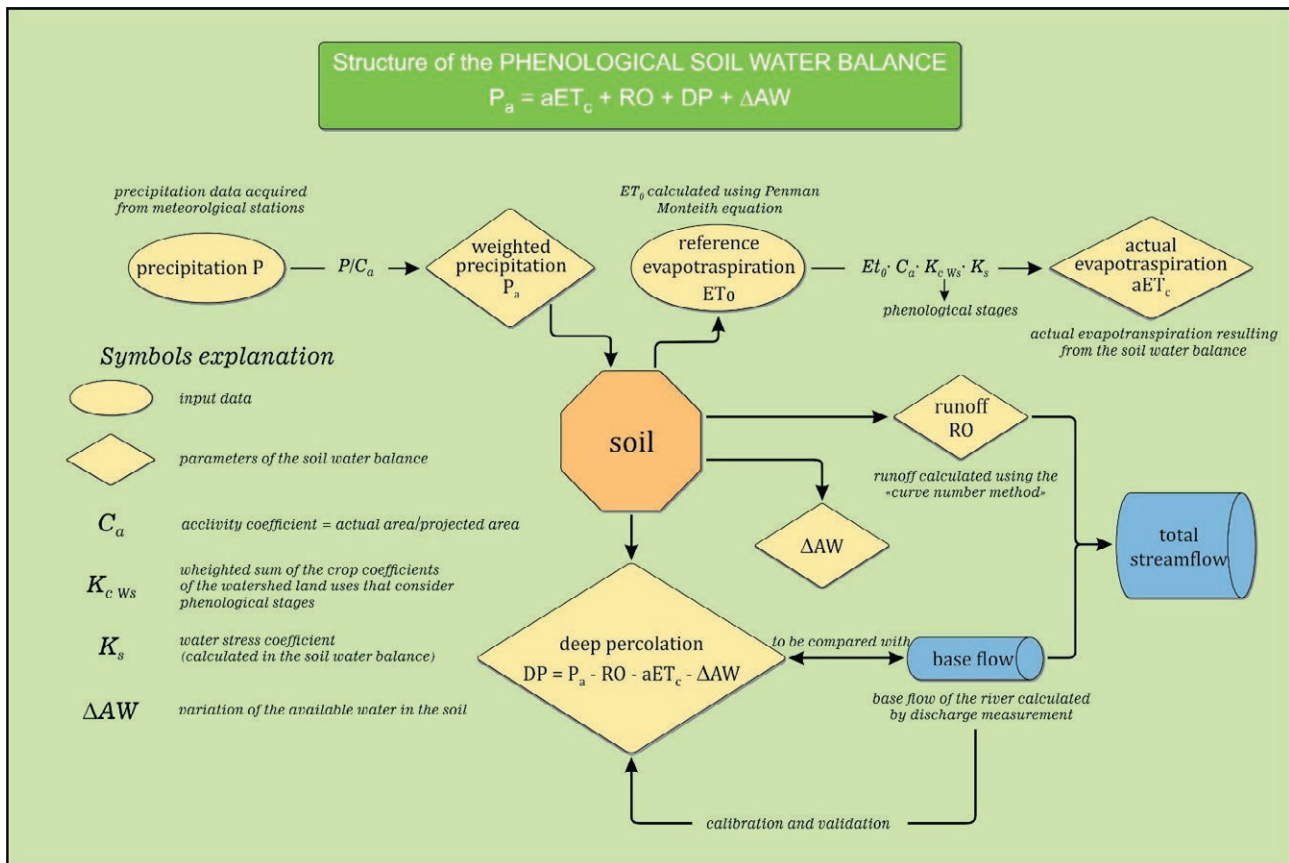


Figure 1.1. phenological soil water balance diagram.

Hydrological models can be mainly distinguished according to:

- 1) the structure (Gayathri et al., 2015): physically based (e.g. SWAT, Neitsch et al., 2011), empirical (e.g. the ones based on Budyko framework, Budyko, 1974), conceptual (e.g. HRU, Becker and Pfützner, 1986);
- 2) the spatial variability of the parameters: lumped (e.g. HEC-HMS, U.S. Army Corps of Engineers, 2013), distributed (e.g. ATHYS, Mishra and Singh, 2003), semi-distributed (e.g. Schumann, 1993);
- 3) how the output values are processed (Farmer and Vogel, 2016): deterministic, stochastic; and
- 4) the calculation time step: daily, monthly, annual etc.

The choice of the most suitable model to use depends on several factors such as the purpose of the study, the scale of application, the geographical region and the availability of the input parameters. Considering the spatial variability of the parameters, in theory distributed and semi-distributed models should perform better than lumped models: this is confirmed by a study of Garavaglia et al., (2017). Anyway, this is not always the case as sometimes lumped models perform equally well or even better than distributed and semi-distributed models (Khakbaz et al., 2012, and references therein, Brirhet and Benaabidate, 2016, and reference therein). Considering calculation time step, daily time step is required for accurate recharge estimates (Dripps and Bradbury, 2007) and so is the most suitable for estimating water resources.

The purpose of our study was to develop, calibrate, apply, and validate a simple but accurate hydrological model that would allow for the accurate estimation of the water resources of a territory, specifically of a watershed.

To achieve this goal, the starting point was the United Nations Food and Agriculture Organization (FAO) Irrigation and Drainage Paper No. 56 (Allen et al., 1998; hereafter 'FAO Paper No. 56') methodology for the dosage of irrigation water for crops, which uses crop coefficients ( $K_c$ ) to calculate potential crop evapotranspiration, taking phenological stages into consideration. To evaluate freshwater availability not only for cultivated areas but for a whole territory, it was necessary to extend this FAO methodology to all land uses. The result is a model that we termed 'phenological soil water balance'.

The phenological soil water balance developed in this work is:

- physically based, as it uses equations to describe the processes and calculate the values of the parameters (equations to calculate the runoff, potential evapotranspiration, etc.);
- lumped, since for each parameter it calculates a single value representative of the spatial variability of that parameter through a weighted sum (e.g.  $K_{c\ ws}$ ,

a unique crop coefficient for the watershed used to compute potential evapotranspiration of agricultural and non-agricultural lands), or as a result of equations in the soil water balance (e.g. the actual evapotranspiration, deep percolation, etc.);

- deterministic, as it treats simulated responses as single, certain estimates of model response without considering randomness; and
- computes a daily time step.

The outline of the model structure is shown in fig. 1.1.

## 2. MATERIALS AND METHODS

### 2.1. Structure of the phenological soil water balance

The following softwares were used to calculate the phenological soil water balance:

- A spreadsheet for the calculation of the values of various parameters (potential reference evapotranspiration, climatic correction of crop coefficients, unique crop coefficient of the watershed, runoff, soil water reserve, etc.), for the processing of the results and their graphical representation.
- A Geographic Information System (GIS) for spatial data analysis and synthesis mapping.

The basic equation of the phenological soil water balance is as follows:

$$P_a = aET_c + DP + \Delta AW + RO \quad (1)$$

where:

$P_a$ : Precipitation corrected with acclivity coefficient. The correction is indicated by the letter (a);

$aET_c$ : actual crop EvapoTranspiration;

$DP$ : Deep Percolation;

$\Delta AW$ : variation of soil Available Water (AW); and

$RO$ : Runoff.

The balance equation is valid for any time interval and for the entire watershed.

For the calculation of the phenological soil water balance it is necessary to determine in advance some parameters that fall directly (e.g.,  $P_a$ ,  $RO$ ) or indirectly (watershed unique crop coefficient  $K_{c\ ws}$ , reference evapotranspiration  $ET_0$ , reference evapotranspiration corrected with the acclivity index  $ET_{0a}$ , average root depth for the calculation of soil water reserve, etc.) in the fundamental equation (eq. 1).

Deep percolation ( $DP$ ) is the unknown of the balance equation, so equation 1 was solved for  $DP$ . To calibrate and validate the balance, the monthly, annual and multi-annual  $DP$  values were compared with the respective baseflow

values, measured at the closing section of the watershed since the baseflow was fed by the deep percolation water.

When comparing monthly and annual totals, the lag time between deep percolation and baseflow, due to the hypogeal path of water, must be taken into account. Deep percolation and baseflow trends were also compared in the calibration.

## 2.2. Flow measurement for baseflow calculation

Flow rates (or discharges) of the stream, with which to calculate the baseflow, were obtained measuring water flows weekly using surface floats (until August 2015) and a hydrometric current meter (from August 2015 to the end of 2019), according to UNI EN ISO 748 (2008). Measures were made at least waiting, after precipitation events, for the watershed runoff time (1,47 hours) before taking the measurement to prevent flow rates from including runoff or hypodermic water flow. Simultaneous measurements were sometimes made between surface floats and current meter: the regression equations found were used to revise the discharge values calculated with surface floats only. Despite this, it is possible that there are uncertainties in some flow measurements from the period up to August 2015.

## 2.3. Required data and step-by-step procedure

### 2.3.1. Required data

Table 2.1 shows the input data necessary to calculate the values of the parameters of the phenological soil water balance.

### 2.3.2. Step-by-step procedure

The procedure that allows the annual elaboration of the phenological soil water balance (eq. 1) consists of the following steps:

1. drafting of the land use map or updating an existing map and calculation of the related areas;
2. calculation of the value of *Curve Number* (CN) for the entire watershed;
3. calculation of daily runoff by the *curve number method*;
4. climatic correction, in the phenological stages, of the cultural coefficients ( $K_c$ ) assigned to the various components of soil use;
5. calculation of the bi-weekly adjusted initial crop coefficient ( $K_{c\text{ ini adj}}$ );
6. calculation of the daily unique crop coefficient for the entire watershed ( $K_{c\text{ ws}}$ );

7. calculation of the daily reference evapotranspiration ( $ET_0$ ) with the Penman–Monteith equation (Allen et al., 1998; Zotarelli et al., 2010);
8. correction for acclivity of daily  $ET_0$  and daily P;
9. calculation of daily potential crop evapotranspiration ( $ET_c$ );
10. calculation of total available water (TAW);
11. calculation of daily rapidly available water (RAW);
12. calculation of daily water stress coefficient ( $K_s$ ); and
13. calculation of deep percolation (eq. 9).

## 2.4. The study area and the acclivity coefficient

### 2.4.1. The study area

The phenological soil water balance was calibrated and validated on the little Santa Maria degli Angeli stream watershed located south of Urbino, Marche Region, central Italy (Fig. 2.1). Considering the IPCC climate classification (IPCC, 2006) the territory belongs to the ‘warm temperate dry’ climate zone.

The watershed is a hilly area with altitudes between 161 and 570 m a.s.l., (average 332 m a.s.l.), with a predominantly agricultural vocation (crops cover about 35% of the territory). It is a sub-watershed in the hydrographic left of the watershed of the Metauro River, which flows into the Adriatic Sea. The main waterstream is called Santa Maria degli Angeli and is 7.6 km long. The watershed has a projected area of 13.451 km<sup>2</sup>. Soil water balance was calculated on a reduced portion of the watershed (Fig. 2.1) as the section on which the water discharges were determined is located about 1 km upstream of the closure of the watershed. This portion has a projected area of 13.098 km<sup>2</sup>.

### 2.4.2. Projected area and Actual area: the acclivity coefficient

In the elaboration of data relative to a territory, the measure of the projected topographic surface (named as “projected area”) is usually considered. In order not to overestimate, for example, the precipitation that effectively falls on a unit surface of soil, it is necessary to consider the actual surface area.<sup>1</sup> This can be obtained in a GIS environment through Digital Terrain Model (DTM) processing and make a correction. This correction can be performed introducing an acclivity coefficient ( $C_a$ ), which is the ratio between the actual area and the projected area:

<sup>1</sup> For a more in-depth discussion of the meaning and application of the concepts “projected area” and “actual area” see supplementary material 1

**Table 2.1.** Input data for phenological soil water balance.

Input data	Application of input data	Source of data for case study
Daily precipitation	Soil water balance, runoff	Weather Observatory “A. Serpieri” of Urbino - meteorological stations of: Urbino, Scientific Campus “E. Mattei, Fermignano (Fig. 2.1). Civil Protection of the Marche Region
Minimum and maximum temperature, minimum and maximum relative humidity, pressure, wind speed, solar radiation (daily)	Reference evapotranspiration $ET_0$	Weather Observatory “A. Serpieri” of Urbino - meteorological stations of: Urbino, Scientific Campus “E. Mattei, Fermignano (Fig. 2.1). Civil Protection of the Marche Region
Base cartography	Digital Terrain Model (DTM) and Triangulated Irregular Network (TIN)	Marche Region, CTR 1:10,000 - sections 279080, 279120, 280050, 280090 <a href="https://www.regione.marche.it/Regione-Utile/Paesaggio-Territorio-Urbanistica">https://www.regione.marche.it/Regione-Utile/Paesaggio-Territorio-Urbanistica</a>
Geology and covers of the watershed	Soil groups for CN calculation	Geological map of Italy 1:50,000, Sheet 279 “Urbino”, Sheet 280 “Fossombrone” <a href="https://www.isprambiente.gov.it/Media/carg/marche.html">https://www.isprambiente.gov.it/Media/carg/marche.html</a>
	Spatialisation of the soil water reserve	PAI Marche 1:10,000 <a href="https://www.regione.marche.it/Regione-Utile/Paesaggio-Territorio-Urbanistica">https://www.regione.marche.it/Regione-Utile/Paesaggio-Territorio-Urbanistica</a>
	Map of infiltration/runoff propensity	Taurino (2004) Gori (2004)
Crop coefficients ( $K_c$ ) of soil uses and duration of phenological stages*	Watershed unique crop coefficient ( $K_{c\ ws}$ )	FAO Paper No. 56 (Allen et al., 1998) WUCOLS IV (Costello and Jones, 2014) Direct observations (phenological stages)
Depth and texture of soil Land use	Computation of the soil water reserve	Soil profile “Mecciano” dug south of Urbino (AA.VV., 2006)
	CN computation	A.G.E.A. ( <i>AGenzia per le Erogazioni in Agricoltura</i> , i.e. Italian Agricultural Payments Agency) aerial orthophotos (2013, 2016)
	Attribution of phenological stages and $K_c$ for the computation of the Watershed unique crop coefficient ( $K_{c\ ws}$ )	Google Earth Pro images
	Map of infiltration/runoff propensity	

\*See tab. 2.3 for values of  $K_c$  and duration of phenological stages.

$$C_a = \frac{aA}{pA} \quad (2)$$

where:

aA: actual Area; and

pA: projected Area.

The coefficient of acclivity is a function of the average slope of the watershed: the greater the average slope, the greater the coefficient of acclivity. In the considered portion of the watershed, with a projected area of 13.098 km<sup>2</sup> and an actual area of 13.979 km<sup>2</sup>, the  $C_a$  is equal to 1.067. The precipitation data are corrected by multiplying them by  $\frac{1}{C_a}$ .

$$P_a = P \cdot \frac{1}{C_a} \quad (3)$$

where:

P: precipitation; and

$P_a$ : precipitation corrected for acclivity.

2.5. Calculation of the potential crop evapotranspiration of the watershed ( $ET$ ) through the watershed unique crop coefficient  $K_{c\ ws}$

2.5.1. The reference evapotranspiration corrected for acclivity ( $ET_{0a}$ )

Evapotranspiration (ET) is the amount of water lost by a soil-vegetation system due to:

- evaporation from the ground and, to a lesser extent, from the surfaces of leaves, trunks, etc.; and
- transpiration of plants.

In the methodology adopted in FAO Paper No. 56 the reference evapotranspiration  $ET_0$ , calculated with

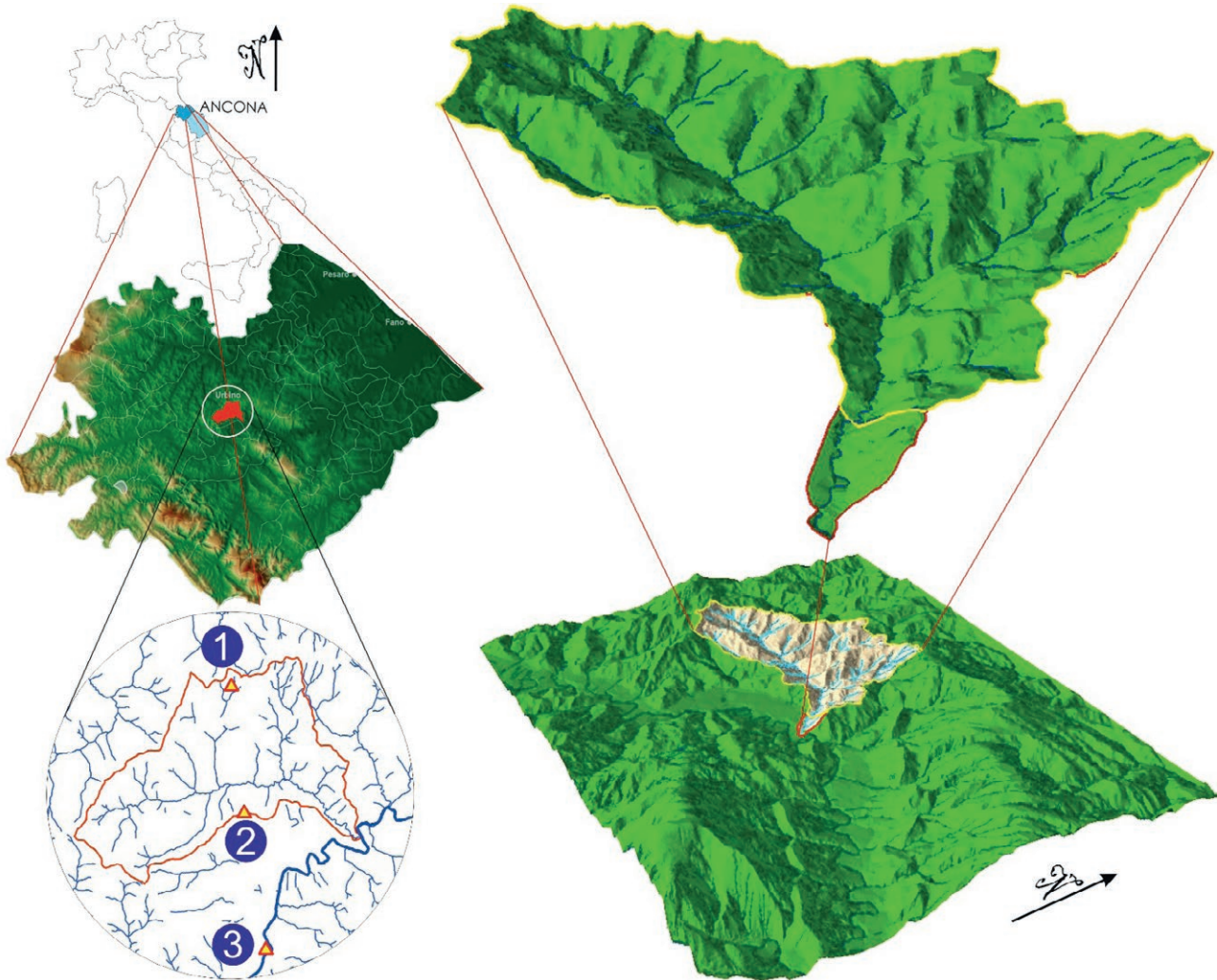


**Figure 2.1.** Location of the Santa Maria degli Angeli watershed study area. 1, Urbino weather station (451 m a.s.l.); 2, Scientific Campus “E. Mattei” weather station (360 m a.s.l.); 3, Fermignano weather station (235 m a.s.l.). The portion of the watershed on which the study was carried out is indicated by the yellow line.

the Penman–Monteith equation, is corrected using the crop coefficient  $K_c$  which is function of the various types of crop and their phenological stages (initial, growing, mid, late), thus obtaining crop evapotranspiration under standard conditions.

As well as for precipitation, the evapotranspiration should also be corrected for acclivity. In this case, however, the effect is the opposite: in fact, considering the projected area, this would produce an underestimation. The  $ET_0$  therefore needs to be multiplied by the acclivity coefficient ( $C_a$ ).

$$ET_{0a} = ET_0 \cdot C_a \quad (4)$$

where:

$ET_0$ : reference evapotranspiration;

$ET_{0a}$ : reference evapotranspiration corrected for acclivity; and

$C_a$ : acclivity coefficient.

However, to obtain an actual hydrological soil water balance, it is necessary to consider the actual evapotranspiration of the territory ( $aET_c$ ). In this study, this parameter was obtained considering, besides the acclivity coefficient, a crop coefficient and a water stress coefficient, each unique to the watershed, which would consider agricultural and non-agricultural land uses.

### 2.5.2. Crop coefficients for agricultural and non-agricultural land use

The crop coefficient ( $K_c$ ) expresses the ratio (eq. 5) between the potential evapotranspiration of a specific crop ( $ET_c$ ) and the reference evapotranspiration ( $ET_0$ ) calculated with the Penman–Monteith equation.

$$K_c = \frac{ET_c}{ET_0} \quad (5)$$

$K_c$  coefficients are used for irrigation water dosing in agriculture. FAO Paper No. 56 reports the crop coefficients of different types of crops and the duration of their relevant phenological stages. Note that such values are to be considered indicative.

Through the crop coefficients the entire watershed  $ET_c$  was calculated, resulting from the values of  $ET_c$  of all the uses of the soil present in the watershed; this was necessary for the calculation of the soil water balance in the period considered.

#### 2.5.2.1. Single crop coefficient $K_c$

In this study, the ‘single crop coefficient’ was adopted, which considers both evaporation from the soil and transpiration from plants (Allen et al., 1998).

$K_c$  varies depending on the type of crop and its phenological stage.

For some crops in FAO Paper No. 56, the duration of the phenological stages is not indicated; in these cases, the durations were assumed based on the durations of similar crops and direct observations.

#### 2.5.2.2. $K_{c\ ini}$ correction and calculation of $K_{c\ ini\ adj}$

In the initial stage of the vegetative cycle, for both annual crops and perennial plant species, evaporation is dominant, also considering that the beginning of the vegetative season coincides with low transpiration and with soils in high water conditions. With the advent of the growing and mid-stage, transpiration prevails, and then returns to the initial relationships at the end of the late season.

The crop coefficient for the initial stage ( $K_{c\ ini}$ ) values, according to FAO paper n. 56, have been calculated for the duration of the initial stage by considering:

1. the time interval between precipitation (or irrigation) events;
2. evaporative power of the atmosphere; and
3. the entity of precipitation events (in relation to infiltration depth and soil texture).

The parameter thus obtained represents the value of  $K_c$  when evaporation prevails; in this study, this parameter was defined as  $K_c$  initial adjusted ( $K_{c\ ini\ adj}$ ) and was calculated over the whole year with a two-week time interval. Two-week trends of  $K_{c\ ini\ adj}$  are shown in figures 2.3, monthly trends in 2.4. It was noted that the drop in precipitation and the increase in  $ET_{0a}$  led to a sharp reduction in the  $K_{c\ ini\ adj}$  in the summer months. This trend was common in all years, although with differences in terms of values such as that of December 2019 (due to low rainfall).

#### 2.5.2.3. Land use classes of the watershed

The phenological soil water balance requires values of  $K_c$  for all uses of the soil of the watershed to calculate, for each year, a single coefficient (referred to as watershed unique crop coefficient,  $K_{c\ ws}$ ) that is the weighted sum of the  $K_c$  for all uses of the soil.

For this purpose, the 2013 land use classes map was created using photointerpretation of aerial orthophotos (A.G.E.A. 2013, see tab. 2.1) and satellite images. The original map is a vector type file hand-drawn and the land use classes are shown in tab. 2.2. The mapping unit was determined by the size of the spatial entities, ranging from the single building (minimal unit) to an extensive forest area (maximal unit). This map was subsequently updated for crops, as they are subject to crop rotation, in the remaining years in which the balance was drawn up (2014–2019). The update was carried out using 2016 A.G.E.A. orthophotos and satellite images, as well as field observations. Arable land (including winter wheat, sunflower, alfalfa, legumes, clover and grapes) and woodland are the most common land use classes.<sup>2</sup>

Land use classes are divided into single classes, consisting of a single component, and mixed classes, consisting of several components. For the latter, however, no  $K_c$  has been defined in the FAO tables. The problem was solved by breaking down these land use classes into basic components, of which the relevant  $K_c$  are given in the literature (Allen et al., 1998, Costello and Jones, 2014) or can be approximated from it. For each mixed class, the percentages of each component are indicated in table 2.2, obtained based on the photointerpretation of aerial orthophotos in the periods considered.

<sup>2</sup> Supplementary material 2 reports the 2013 land use map and the distribution of land use class areas within the Santa Maria degli Angeli watershed

**Table 2.2.** Land use classes and components of land use classes, with the percentage by which the components form the classes.

Land use classes	Components of land use classes	Percentage of components in each of the land use classes
Totally waterproof areas	Waterproof	100%
	Waterproof	35%
Area near built-up	Herbaceous species	30%
	Shrubs/small trees	15%
	Trees	20%
Arable land with wheat	Wheat	100%
Arable land with sunflower	Sunflower	100%
Arable land under fodder crops (alfalfa)	Forage (alfalfa)	100%
Arable land in legumes	Faba bean	100%
Arable land with clover	Clover	100%
Vineyard	Vineyard (vine)	100%
Set-aside land	Herbaceous Oats	50%
	species Mint	50%
Uncultivated	Herbaceous species	45%
	Broom	35%
	Shrubs/small trees	10%
	Trees	10%
Sparse woods	Herbaceous species	20%
	Broom	15%
	Shrubs/small trees	15%
	Trees	50%
Woods	Herbaceous species	10%
	Broom	5%
	Shrubs/small trees	10%
	Trees	75%

#### 2.5.2.4. Phenological stages and relative crop coefficient for all land use components

Table 2.3 shows the values of the crop coefficient for all land use components, the crop sowing period, and the start and end dates of each phenological stage, obtained by adapting the FAO Paper No. 56 values to the context of the study area or by calculating *ex novo* the crop coefficients of the mixed land use classes. In the notes to the table, the criteria for the attribution of the values of the  $K_c$  are shown. The crop coefficients must be corrected for average moisture and wind speed conditions, in the mid and late stages, using appropriate equations given in FAO paper No.56.

The scheme of Fig. 2.2 graphically reports the durations of the phenological stage of all the components of land use.

#### 2.5.2.5. $K_{c,actual}$

The daily values of  $K_c$  for each land use component (Table 2.3) were compared with the values of  $K_{c,ini,adj}$ .

$K_c$  mainly depends on the transpiration of the plants while  $K_{c,ini,adj}$  exclusively represents evaporation from the soil surface. In the dormancy periods,  $K_{c,ini,adj} > K_c$ , while in periods of greater vegetative development (usually the spring and summer months),  $K_c > K_{c,ini,adj}$ . To avoid underestimating the evapotranspirative demand, it is necessary to adopt the higher value of the two. This value is the  $K_{c,actual}$  and can be calculated for both single (e.g. winter wheat, Fig. 2.3) and mixed (e.g. wood) land use classes.

#### 2.5.2.6. Watershed unique crop coefficient ( $K_{c,ws}$ ) and calculation of watershed potential crop evapotranspiration ( $ET_c$ )

For each day of the year, the weighted sum of the daily values of the various  $K_{c,actual}$  of the single and mixed land use classes was calculated. In this way, a single value for the entire watershed was obtained—the unique watershed crop coefficient ( $K_{c,ws}$ )—which varies with phenological stages. The equation is as follows:

$$K_{c,ws} = \sum_{j=1}^n \frac{area_{land\ use\ j}}{area_{watershed}} \cdot K_{c,actual\ land\ use\ j} \quad (6)$$

where:

$K_{c,ws}$ : daily unique watershed crop coefficient;

area land use j: total area of a given land use class in the year under consideration. The values of j, from 1 to n, refer to each of the various classes identified in the watershed; and

$K_{c,actual\ land\ use\ j}$ : daily  $K_{c,actual}$  of a given land use class (see par. 2.5.2.5) based on its phenological stage. The values of j, from 1 to n, refer to each of the various classes identified in the watershed.

The value of  $K_{c,ws}$ , therefore, indicates how much the maximum daily evapotranspirative demand of the entire watershed (and not of a single crop or component or class) differs from that of reference  $ET_{0a}$ .

Figure 2.4 a and b show the monthly performance of the  $K_{c,ws}$  in the last 2 years of the water balance. The constant value (equal to 1) of the reference coefficient ( $K_{c,ref}$ ), which is the value of the coefficient of the reference crop (a grass meadow/fescue maintained in optimal water conditions), is also reported. The values of  $K_{c,ini,adj}$  and the weighted sum of the watershed land use coefficients ( $K_c$ ) are also given as a comparison. It should be



**Table 2.3.** Components of the land use classes and  $K_c$  values adopted for each of the phenological stages. The dates of the beginning, end and duration of the phenological stages, the duration of the entire vegetative cycle, the FAO region to which the values refer (from FAO Paper No. 56, modified) are also reported. Impermeable soil:  $K_c = 0$ . Values of crop coefficients, in the mid and late stage, were corrected for relative humidity and wind speed as indicated by FAO Paper No. 56.

Component	Stage						FAO Region FAO sowing date <i>Local sowing date</i>
	Initial	Growing <sup>1</sup>	Mid	Late <sup>2</sup>	Non vegetative stage <sup>3</sup>	Duration of vegetative cycle (days)	
Winter wheat	Number of days	30	140	40	30	125	Mediterranean November 15 November
	Period	15nov-14dec	15dec-03may	04may-12jun	13jun-12jul	13jul-14nov	
	$K_c$ value	0.7	0.7→1.15	1.15	1.15→0.25	$K_{c,ini}$ adj	
Sunflower	Number of days	25	35	45	25	235	Medit./Calif. April/May 01 May
	Period	01may-25may	26may-29jun	30jun-13aug	14aug-07sept	08sept-30apr	
	$K_c$ value	0.35	0.35→1.05	1.05	1.05→0.35	$K_{c,ini}$ adj	
Legumes (faba bean) <sup>4</sup>	Number of days	90	55	47	43	130	Europe November 01 November
	Period	01nov-29jan	30gen-24mar	25mar-11may	12may-22jun	23jun-31oct	
	$K_c$ value	0.5	0.5→1.15	1.15	1.15→0.35	$K_{c,ini}$ adj	
Clover <sup>5</sup>	Number of days	160	41	31	22	111	Not present in FAO Paper No. 56 01 November
	Period	01nov-09apr	10apr-20may	21may-20jun	21jun-12jul	13jul-31oct	
	$K_c$ value	0.4	0.4→1.15	1.15	1.15→0.4	$K_{c,ini}$ adj	
Vineyard <sup>6</sup>	Number of days	30	60	40	80	155	Mid latitudes (wine)
	Period	01apr-30apr	01may-29jun	30jun-08aug	09aug-27oct	28oct-31mar	
	$K_c$ value	0.3	0.3→0.7	0.7	0.7→0.45	$K_{c,ini}$ adj	
Alfalfa <sup>7</sup>	Number of days	10	20	115	5	215	California (USA) Jan-Apr (last -4°C) 01 apr (1 <sup>st</sup> year)
	Period	01apr-10apr	11apr-30apr	01may-23aug	24aug-28aug	29aug-30mar	
	$K_c$ value	0.4	0.4→0.95	0.95	0.95→0.9	0.4	
Oat <sup>8</sup>	Number of days	40	30	40	20	235	Not specified
	Period	05mar-13apr	14apr-13may	14may-22jun	23jun-12jul	13jul-04mar	
	$K_c$ value	0.35	0.35→1.15	1.15	1.15→0.25	$K_{c,ini}$ adj	
Mint <sup>9</sup>	Number of days	80	40	50	40	155	
	Period	01jan-21mar	22mar-30apr	01may-19jun	20jun-29jul	30jul-31dec	
	$K_c$ value	0.6	0.6→1.15	1.15	1.15→0.6	0.6	
Shrubs <sup>10</sup> (sp.broom or cytissus)	Number of days	75	45	75	45	125	
	Period	01jan-16mar	17mar-30apr	01may-14jul	15jul-28aug	29aug-31dec	
	$K_c$ value	0.15	0.15→0.35	0.35	0.35→0.15	0.15	
Little trees/ brushes	Number of days	90	45	130	30	70	
	Period	01jan-31mar	01apr-15may	16may-22sept	23sept-22oct	23oct-31dec	
	$K_c$ value	0.50	0.50→0.90	0.90	0.90→0.65	0.65→0.5	

(Continued)

Table 2.3. (Continued).

Component	Stage						FAO Region FAO sowing date <i>Local sowing date</i>
	Initial	Growing <sup>1</sup>	Mid	Late <sup>2</sup>	Non vegetative stage <sup>3</sup>	Duration of vegetative cycle (days)	
Trees <sup>11</sup>	90	45	130	40	60	365	
Number of days							
Period	01jan-31mar	01apr-15may	16may-22sept	23sept-01nov	02nov-31dec		
K <sub>c</sub> value	0.5	0.5→1.2÷1.3	1.2÷1.3	1.2±1.3→0.65	0.65→0.5		

<sup>1</sup> The value is proportional between  $K_{c,ini}$  and  $K_{c,mid}$  (the formula is given in FAO Paper No. 56, chapter 6, equation 66).

<sup>2</sup> Is the final value. During the late stage the value is proportional between  $K_{c,mid}$  and  $K_{c,end}$  (the formula is given in FAO Paper No. 56, chapter 6, equation 66).

<sup>3</sup> For crops with a growing cycle of less than one year, the adjusted initial coefficient  $K_{c,ini,adj}$  is applied in the months when the crop is not present.

<sup>4</sup> The value of  $K_{c,end}$  was increased from 0.3 to 0.35 because at harvest the *faba bean* had not yet reached the end of the vegetative cycle for climatic reasons.

<sup>5</sup> FAO individual cutting period. Since the clover is collected for seed in the watershed, the value of  $K_{c,end}$  of FAO Paper No. 56 was not considered suitable, as it is a pre-cut value (1.10). It was considered more correct to attribute a  $K_c$  value of 0.4.

For the clover, FAO Paper No. 56 does not indicate the phenological stage, which have been hypothesised based on direct observations.

<sup>6</sup> FAO grapes, wine. The vineyard is a perennial plant but in periods when there is no vegetative cycle the soil between the rows is tilled. Consequently, in the periods of the year when there is no vegetative cycle of the vine, the initial adjusted coefficient  $K_{c,ini,adj}$  was used.

<sup>7</sup> The 'averaged cutting effects' typology was adopted; that is, a single cycle that averages all the cutting cycles of the crop. After the last cut, for the dormancy period, it assumed the value of  $K_{c,ini,adj}$ .

<sup>8</sup> Although not cultivated in the territory of study, in the wild variant it goes to form 50% of the 'grass' component of the set-aside soils. The value of  $K_{c,ini}$  was assumed here to be 0.35 by analogy with other cereals. The duration of the phenological stage was obtained from FAO Paper No. 56 without Region specification.

<sup>9</sup> Multiannual plant. Even if not cultivated in the territory of study, in the wild variant it goes to form 50% of the 'grass' component of the set-aside soils. The  $K_{c,end}$  of FAO Paper No. 56 is 1.10 but it is a pre-cut value; in this study, it was assumed to be 0.6 because it considers mint as a multi-annual spontaneous grass that is not harvested. The duration of the phenological stage was obtained from direct observations and by analogy with other herbaceous species reported in FAO Paper No. 56.

<sup>10</sup> Includes all shrubs (smoke bush, wild blackthorn, etc., except brooms) and small trees (elder, small elms, wild cherry, etc.). For the definition of the  $K_c$  values, the values of FAO Paper No. 56 were used, using the values of the crops with characteristics most like the species of this group. The duration of the phenological stage was considered to coincide with that of the trees. For the winter dormant stage, a value of 0.5 was assumed, equal to the value of the initial stage. This value is relative to the months from January to the beginning of the vegetative stage; from the end of the 'late' stage to 31 December there is a second stage ('late 2') in which  $K_c$  drops from 0.65 to 0.5, also characteristic of the component 'wood'.

<sup>11</sup> The duration of the phenological stage of the component 'trees' was deduced by adapting the work of Eccel et al., 2007, which reported the trend of  $K_c$  and LAI for an alpine deciduous forest, to the context of the Santa Maria degli Angeli watershed. Values of  $K_c$  were computed using the formulas of the FAO paper No.56, chapter 9, adapted to the context of the study area. The maximum value of  $K_c$  is variable because a parameter value needs to be calculated that accounts for evaporation based on the frequency of rain events (or wet soil) during the mid-season. The symbol ÷ in this case does not represent division but is intended to signify that the value varies between 1.2 and 1.3 depending on the parameter mentioned.

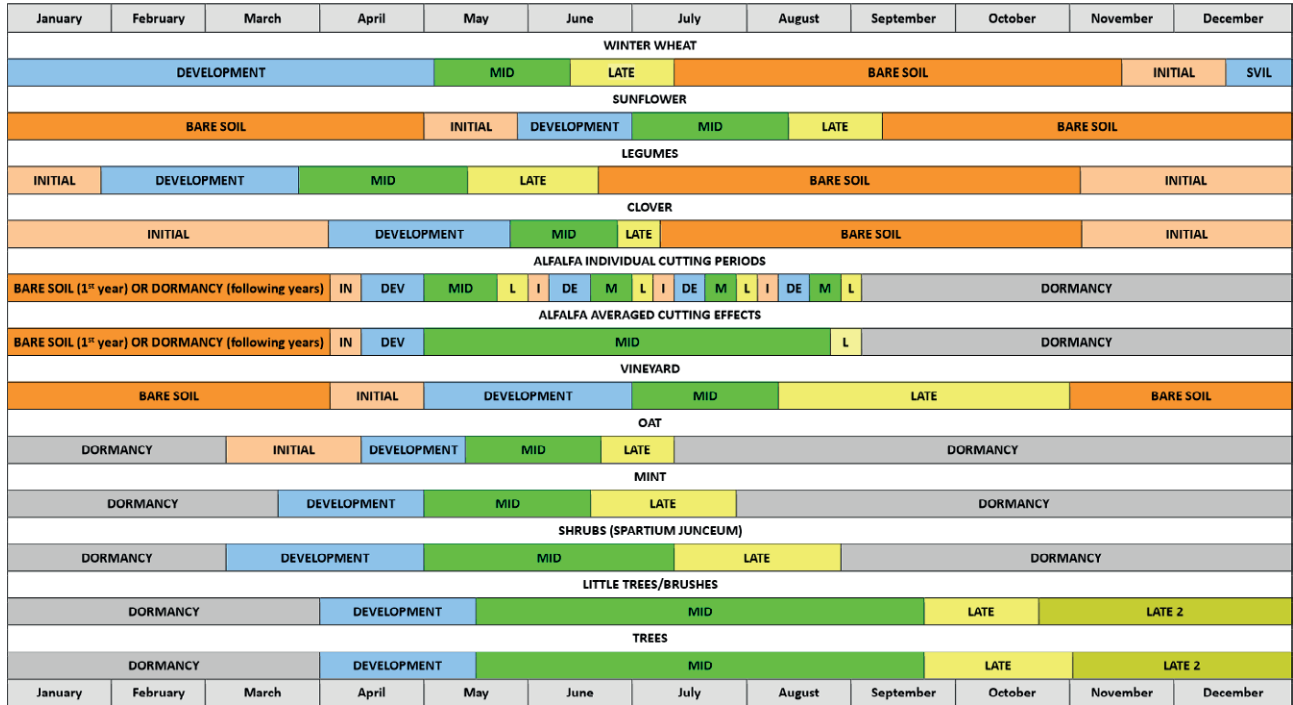


**Figure 2.2.** Duration of the phenological stages of the components that form the land use classes present in the Santa Maria degli Angeli watershed. The ‘development’ stage corresponds to the ‘growing’ stage in table 2.3.

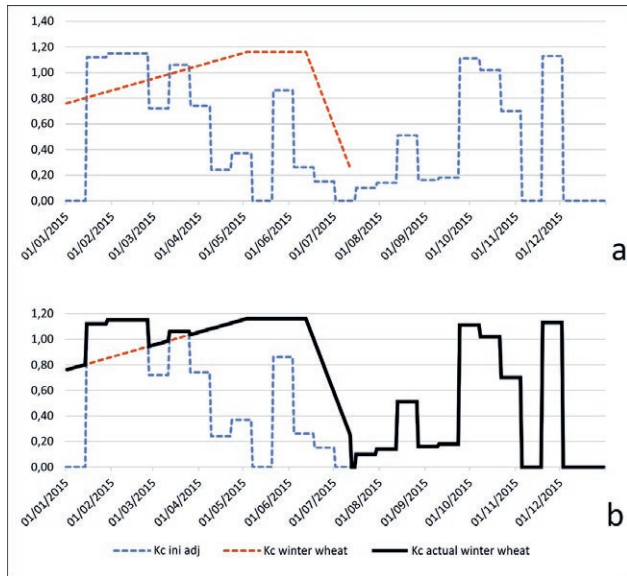


**Figure 2.3.** Winter wheat single land use class. a) trend of  $K_c$  and  $K_{c\ ini\ adj}$  in the year 2015; b) trend of  $K_{c\ actual}$  in the year 2015 obtained as the highest of the values of  $K_c$  and  $K_{c\ ini\ adj}$ .

noted that the parameter  $K_{c\ ws}$  assumes higher values when the value of evaporation ( $K_{c\ ini\ adj}$ ) or transpiration ( $K_c$ ) is high.

The  $K_{c\ ws}$  weights the two effects and provides a representative value of the territory from the values of the coefficients and phenological stages of all the land use classes. Although the values are different from year to year, the trends are similar. It was observed that the  $K_{c\ ws}$  almost never exceeds the  $K_{c\ ref}$ , so the potential evapotranspirative demand of the territory is almost always lower than the theoretical one of the reference crop.

$K_{c\ ws}$ , therefore, represents the parameter whose value is to be multiplied by the reference evapotranspiration corrected for the coefficient of acclivity ( $ET_{0a}$ ) to obtain the potential crop evapotranspiration of the watershed ( $ET_c$ ). The equation is as follows:

$$ET_c = ET_{0a} \cdot K_{c\ ws} \tag{7}$$

where:

$ET_c$ : maximum potential ‘crop’ evapotranspiration of the watershed (mm);

$ET_{0a}$ : potential evapotranspiration corrected by the coefficient of acclivity (mm); and

$K_{c\ ws}$ : daily unique crop coefficient of the entire watershed.

Estimating crop evapotranspiration ( $ET_c$ ) is crucial for ensuring sustainable and efficient agricultural water

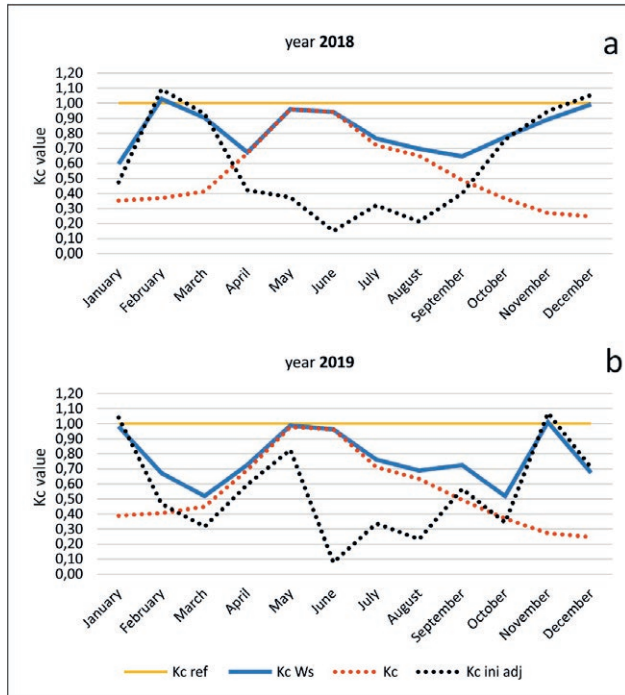


**Figure 2.4.** Trend of the watershed unique crop coefficient ( $K_{c,ws}$ ) in the last two years of the water balance. The  $K_c$  trends obtained only from the values of Table 2.3, of the adjusted initial coefficient ( $K_{c,ini,adj}$ ) and of the  $K_c$  of the reference crop ( $K_{c,ref}$ ) are also reported.

management (Barrera et al., 2023) and is therefore also important in water management of the whole watershed.

Finally, to obtain the actual evapotranspiration it is necessary to calculate the water stress coefficient ( $K_s$ ), which is calculated inside the phenological soil water balance.

## 2.6. Calculation of actual evapotranspiration ( $aET_c$ )

Another parameter of the phenological soil water balance is represented by the variation of the water reserve of the soil.  $K_s$  is a coefficient denoting the state of soil water stress and is a function of total available water (TAW), rapidly available water (RAW) and soil water depletion (Dr) (Allen et al., 1998). When  $K_s = 1$  there is no water stress. If  $K_s < 1$  there is water stress.

These parameters were calculated based on a ‘Mecciano’ soil profile performed inside the watershed (AA.VV., 2006). The TAW of the ‘Mecciano’ soil profile was then spatially extended to consider the variability of thicknesses and soil types. This resulted in a TAW unique to the basin and used in the balance, which is the result of a weighted sum over three different conditions deriving from the crossing between land use and geology. At each

of these condition a share of the TAW of the ‘Mecciano’ soil profile is assigned: the entire TAW value for thick soils (arable land on cover deposits), half a value for thin soils (non-arable land on rocky substrate), an intermediate value for soils of intermediate thickness (arable land on rocky substrate).

The actual evapotranspiration of the watershed of the day,  $aET_c$ , is a function of  $ET_c$  according to the coefficient of water stress  $K_s$  (Allen et al., 1998):

$$aET_c = ET_c \cdot K_s \quad (8)$$

where:

$aET_c$ : actual watershed evapotranspiration (mm);

$ET_c$ : potential maximum ‘crop’ evapotranspiration of the watershed (mm) (eq. 7); and

$K_s$ : unique water stress coefficient for the entire watershed.

## 2.7. Calculation of runoff<sup>3</sup>

For the calculation of the daily values of the runoff parameter, which contribute to the phenological soil water balance (see eq. 1), the curve number methodology (Mockus, 1972; USDA, 2004), with its subsequent modifications (Williams et al., 2000; Williams et al., 2005; Kannan et al., 2008; Williams et al., 2012; Friuli Venezia Giulia Autonomous Region, 2018), was used.

## 2.8. Determination of deep percolation through soil water balance

Based on the methodology described above, the values of the parameters of the phenological soil water balance were calculated daily, excluding the deep percolation (DP) value, which remained unknown.

To derive this unknown, the equation (1) was solved as follows:

$$DP = P_a - RO - aET_c - \Delta AW \quad (9)$$

where:

DP: Deep Percolation;

$P_a$ : daily precipitation corrected with the acclivity coefficient;

RO: daily runoff;

$aET_c$ : daily actual crop evapotranspiration; and

$\Delta AW$ : daily variation of soil Available Water (AW).

<sup>3</sup> Insights into the methodology adopted, together with the calculation of runoff in significant periods of the year 2015, can be found in supplementary material 3.

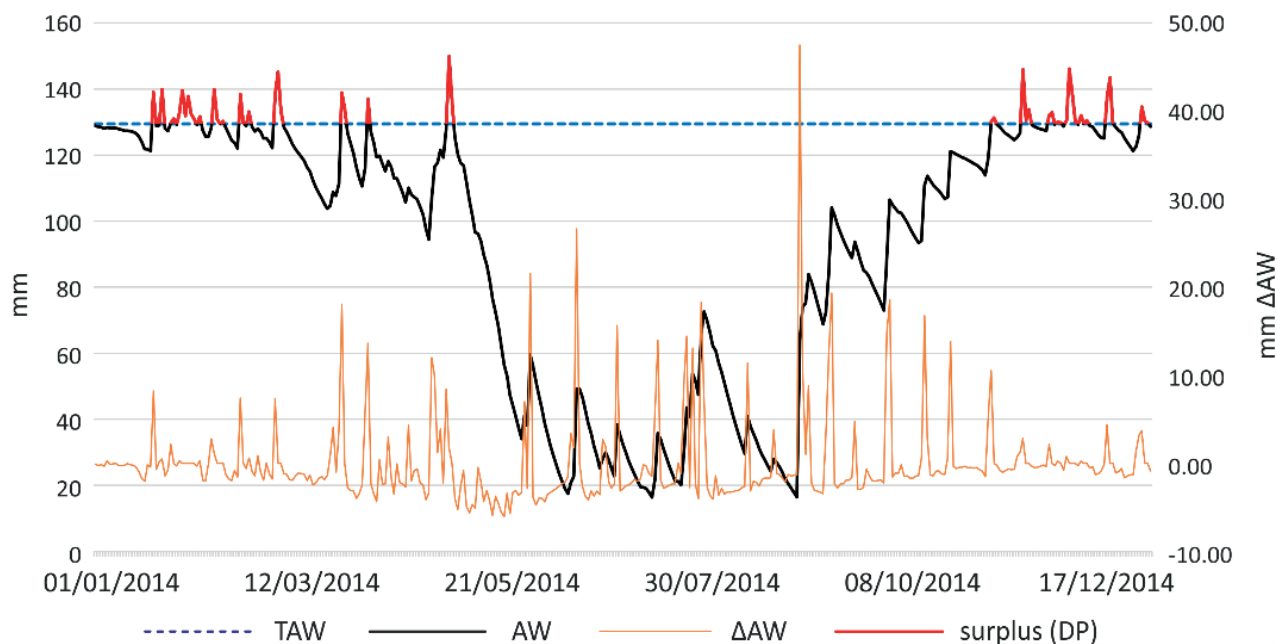


**Figure 2.5.** Daily trend of available water (AW), variation of available water ( $\Delta$ AW) and surplus/deep percolation in the year 2014 in the soils of Santa Maria degli Angeli watershed. The total available water (TAW) value is also reported.

It should be noted that there is deep percolation only when there is surplus; that is, AW reaches the maximum value which is represented by the total available water (TAW) and then  $\Delta$ AW = 0 (Fig. 2.5). The water that goes into deep percolation reaches the aquifers and hence the lower and main hydrographic network.

### 2.9. Calibration and validation of the model

To verify whether the model worked well, the values of deep percolation thus obtained were compared with the baseflow values deriving from flow measurements at the closing section of the watershed. The baseflow is determined by the water of the deep percolation that, after a hypogeal path, feeds the stream. The soil water balance model was calibrated in 2013 and validated in the next 3 years (2014, 2015, 2016). The last years (2017, 2018, 2019) provided further confirmation of the validity of the model.

To also make a qualitative comparison with the deep percolation, the trends in the levels of groundwater were investigated. Piezometric levels were measured in four watershed aquifers, in different hydrogeological contexts and at different depths: two shallower, and two deeper. The measurements were performed on the same dates as those of flow measurements.

**Table 2.4.** Values of the Pearson and KGE statistical indices for the calibration and validation period of the model.

	Pearson	Kling-Gupta Efficiency
Calibration period (2013)	0,74	0,57
Calibration + validation period (2013-2016)	0,75	0,69

**Table 2.5.** Totals of the baseflow and deep percolation values for the calibration and validation period of the model.

Period	Baseflow totals (mm)	Deep percolation totals (mm)	Percent change (%)
Calibration period (2013)	274	279	+2
Calibration + validation period (2013-2016)	986	877	-11

### 2.10. Statistical analysis on the calibration and validation of the model

The time lag between deep percolation and baseflow makes it necessary to pay attention to a statistical comparison, as deep percolation values calculated in one month may find corresponding (not equal) values one or more months later.

The sets<sup>4</sup> of monthly baseflow (measured/observed) and deep percolation (forecast/simulated) values for the calibration and validation period 2013-2016 were analysed using the Pearson index and KGE index (Gupta et al., 2009). The results are reported in Table 2.4.

Knoben et al. (2019) demonstrate that KGE values greater than -0.41 indicate that a model improves upon the mean flow benchmark even if the model's KGE value is negative; KGE = 1 indicates perfect agreement between observations and simulations. The values of the indices in tab. 2.4 provide a fair correlation, but as mentioned above, they are not entirely suitable for assessing the goodness of the model. Given the hydrological processes, a comparison with an index analysing multi-annual totals seems more appropriate. In Table 2.5 are the percentage changes between deep percolation and baseflow annual and multi-annual totals over the calibration and validation period.

The 11% difference, an acceptable value, between the multi-annual totals confirmed the validity of the phenological soil water balance model.

Table 3.2 in the results section shows the percent change that also considers the last years in which the balance was calculated.

### 3. RESULTS

Results obtained by applying phenological soil water balance, comparison with measured base flow and calculation of watershed water deficit are discussed below.

#### 3.1. Annual values of the parameters of the phenological soil water balance

Table 3.1 gives the total annual values of deep percolation (DP) from the phenological soil water balance (eq. 9) for the seven years of the study<sup>5</sup>. The  $\Delta AW$  parameter, which indicates the changes in the amount of water available in the soil over a period of one year, had a minimal variation since the water reserve was reconstituted at the end of each year.

**Table 3.1.** Total annual values, expressed in mm, of the parameters of the phenological soil water balance (eq. 9), where DP = deep percolation,  $P_a$  = precipitation corrected for acclivity, RO = runoff,  $aET_c$  = actual evapotranspiration and  $\Delta AW$  = variation of the available water.

year	$DP = P_a - RO - aET_c - \Delta AW$				
	DP	$P_a$	RO	$aET_c$	$\Delta AW$
2013	279.1	1022.2	144.2	599.4	-0.6
2014	245.0	1067.3	148.1	674.5	-0.3
2015	210.5	850.8	116.5	528.5	-4.7
2016	142.4	833.9	78.8	614.0	-1.3
2017	157.0	752.1	71.7	518.1	5.3
2018	251.3	857.3	74.6	537.2	-5.8
2019	113.3	803.1	60.6	625.8	3.3

#### 3.2. Comparison of deep percolation with the measured baseflow<sup>6</sup>

Fig. 3.1 shows the monthly values of deep percolation, baseflow and the piezometric level of the aquifers in the 4 years of phenological soil water balance in which the calibration and validation of the model were carried out. Precipitation values are also reported.

The graph shows a correspondence between the trend of deep percolation and baseflow in both decreases and increases. However, the rise of the baseflow occurs later than the deep percolation; the observed delay time corresponds to the time needed for the hypogeous water path.

The extent of the delay depends on the characteristics of the watershed (size, geology-geomorphology, structural layout, thickness, texture and permeability of soils, slopes, land use, etc.).

The starting value of the virtual aquifer was obtained from the average of the initial levels of the four considered aquifers; its subsequent evolution was calculated based on the average of the percent changes in each aquifer.

A comparison between deep percolation and baseflow in the different years (Table 3.2) allowed for evaluation of the accuracy of the model in simulating the processes that take place in the water cycle of the territory. To annual period there is a lower correspondence between the two parameters: as previously written this is due to the delay time of the hypogeous path of the percolation water, which postpones to the first months of the following year the effect of precipitation falls in the last months of the year; in a multi-annual period the two parameters must have comparable values, otherwise the model does will not perform well. It was noted that in

<sup>4</sup> All monthly DP and baseflow values (2013-2019) are given in supplementary material 4

<sup>5</sup> An example of the application of the phenological soil water balance in significative periods of the years 2014, 2015 and 2016 is set out in supplementary material 5

<sup>6</sup> All monthly values of the phenological soil water balance are given in supplementary material 6

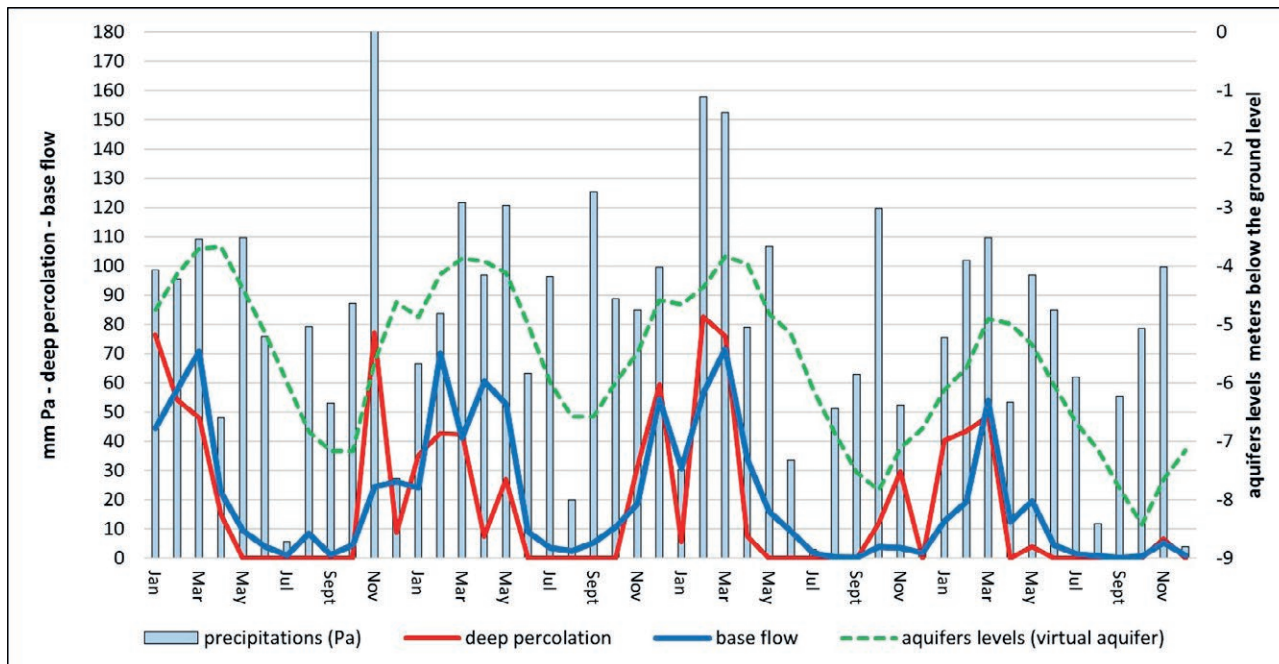


**Figure 3.1.** Comparison between the trends of the precipitations ( $P_a$ ), deep percolation (DP), baseflow and aquifer levels (expressed through the trend of a virtual aquifer representing the trend of the levels of 4 monitored aquifers) from the years 2013 to 2016. For reasons of scale, the  $P_a$  value of november 2013 was cut (original value: 232,7 mm).

**Table 3.2.** Total annual values of the deep percolation derived from the phenological soil water balance model and the baseflow measured at the closing section of the watershed. Values are rounded to the nearest unit.

year	measured base flow (mm)	deep percolation (mm)	percent change (%)
2013	274	279	+2
2014	352	245	-30
2015	228	213	-7
2016	131	141	+8
2017	104	157	+51
2018	235	251	+7
2019	120	113	-6
sum	1444	1400	-3
mean	206	200	-3

some years the difference between the values could also be quite significant (in 2014 and 2017) but at a multi-annual level both the sum and the average of the values differed by a very low percentage value, signifying the good performance of the model.

The graph in Fig. 3.2 shows the average values at 10 days of runoff, deep percolation and precipitation in the period 2013–2019, useful for the estimation of the water resources of the Santa Maria degli Angeli watershed.

The mean decadal precipitation was 49 mm, resulting in a runoff of 5.4 mm (corresponding to 75970 m<sup>3</sup> of water) and a deep percolation of 10.9 mm (corresponding to 152995 m<sup>3</sup> of water).

Obviously, in the summer months there are few or no runoff and deep percolation, while the recharge of the aquifers and the rise of the baseflow (effect of the deep percolation) is maximal in the winter period.

### 3.3. Water deficit of the watershed

The graph in Fig. 3.3 reported the multi-annual average to 10 days time step of some parameters of the phenological soil water balance and the  $K_{cws}$  throughout the study period (2013–2019).

The study allowed for quantification of the water deficit at the level of the entire watershed as the difference between  $ET_c$  and the actual evapotranspiration ( $aET_c$ ), thus enabling the evaluation of the water stress during the year. Water deficit is graphically expressed by the distance between the curves representing these two parameters. The greater the distance between the two curves (indicated with a red arrow), the greater the deficit. The red arrow highlights the extent of the water deficit. The average annual value of the 2013–2019 deficit was 282 mm (about 4·10<sup>6</sup> m<sup>3</sup> of water).

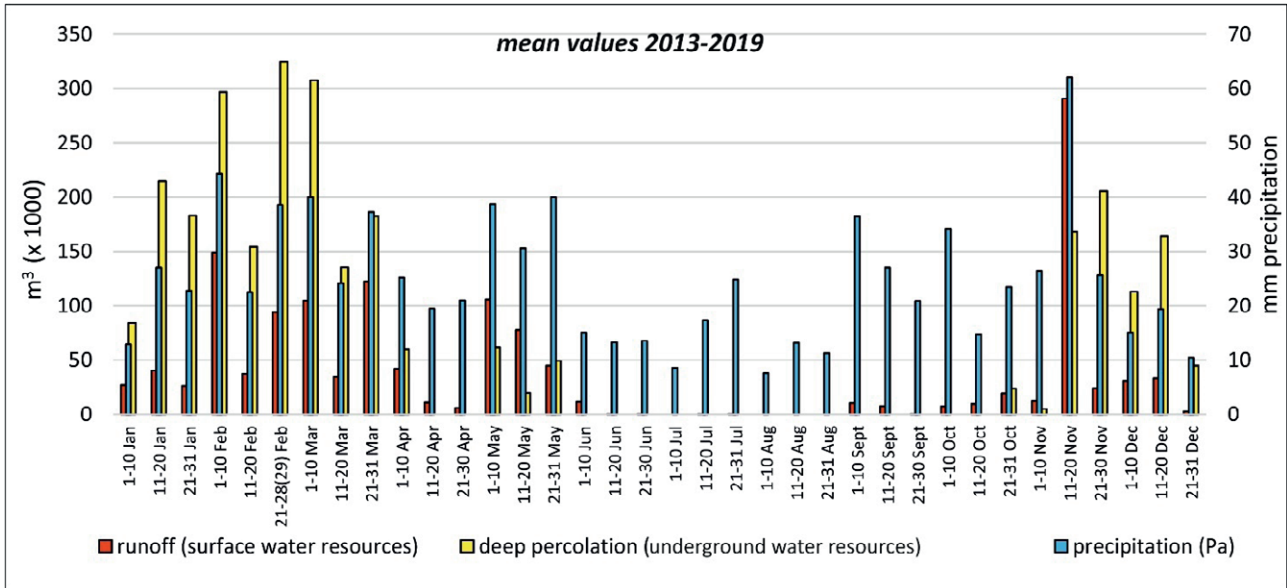


Figure 3.2. Multi-annual average to 10-day time step of the values of precipitation, runoff and deep percolation of the Santa Maria degli Angeli watershed.

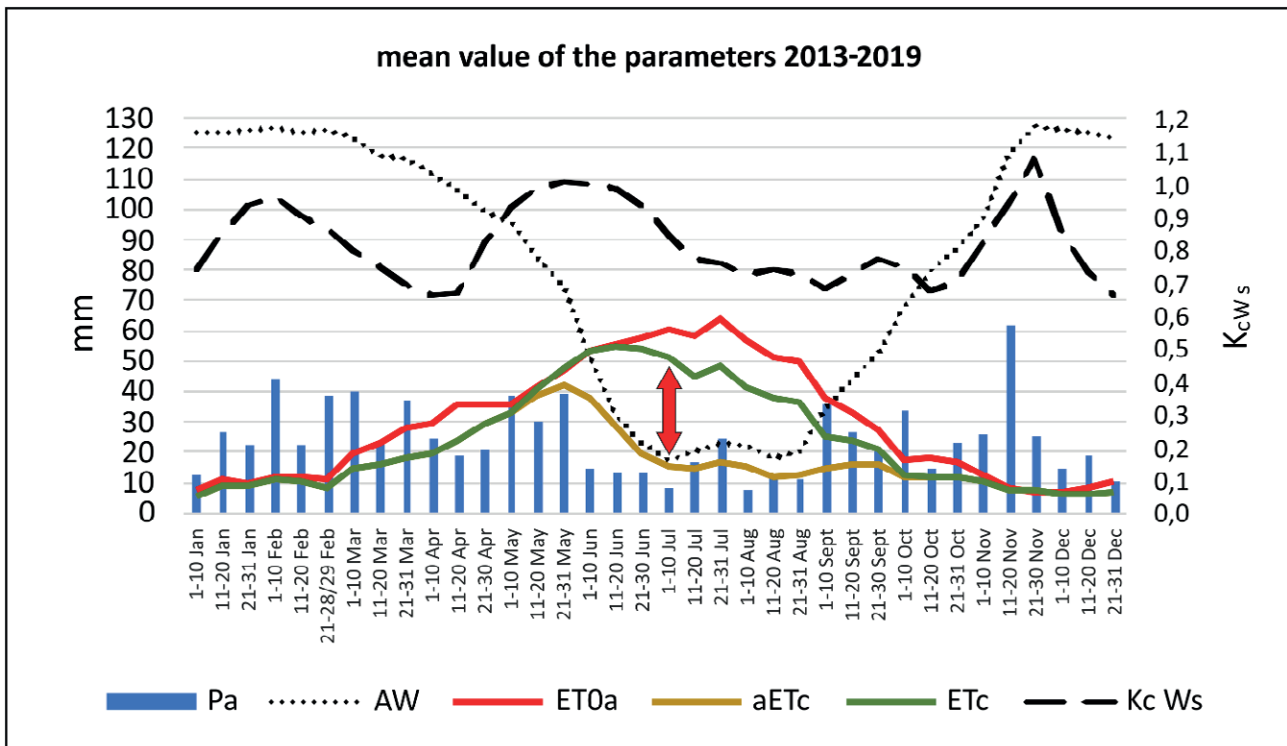


Fig. 3.3. Multi-annual mean values at 10-day time step of the parameters of the phenological soil water balance model used for the calculation of the water deficit (difference between  $ET_c$  and  $aET_c$  highlighted by the red arrow).  $P_a$ : precipitations weighted for acclivity. AW: soil water reserve.  $ET_{0a}$ : reference evapotranspiration weighted for acclivity.  $aET_c$ : actual evapotranspiration.  $ET_c$ : potential crop evapotranspiration.  $K_{cWs}$ : unique watershed crop coefficient. All parameters are referred to the whole watershed.



During the seven years in which the phenological soil water balance was calculated, 2014 was the year with the lowest deficit (186 mm, corresponding to  $2.6 \cdot 10^6 \text{ m}^3$  of water while 2017 was the year with the greatest deficit (472 mm, corresponding to  $6.6 \cdot 10^6 \text{ m}^3$  of water;). The month for which the highest deficit value was recorded was June 2016, with a deficit of 172 mm, corresponding to  $2.4 \cdot 10^6 \text{ m}^3$ , which almost equals the entire annual deficit of the year 2014.

#### 4. DISCUSSION

The above results demonstrate that detailed studies of water resource management in agriculture (that use crop coefficients in the context of irrigation and applications) can also be applied at the level of the entire watershed or for an administrative entity.

The advantage of this approach that extend to whole watershed the crop coefficients methodology (and so the phenological stages of crops/plant varieties) is the accurate calculation for all land uses, through the watershed unique crop coefficient  $K_{c_{ws}}$ , of the parameters of maximum crop evapotranspiration ( $ET_c$ ) and consequently of actual evapotranspiration ( $aET_c$ ).

The latter is a key parameter in soil water balance. As a consequence of this it is possible to develop a soil water balance capable of accurately calculating deep percolation, from which the baseflow trend can be approximated, after considering the lag time between the two caused by the time taken by the water to complete its underground path. Baseflow values provides the estimate of potential water resources.

In addition, from the difference between the two evapotranspiration parameters, the deficit of the entire watershed can be calculated.

In order to achieve this type of model, the study combined the design of a theoretical hydrological model related to soil water balance with field monitoring by surveying flow rates and piezometric levels of aquifers. The monitoring of the flow rates of the main stream allowed the model to be calibrated and validated, comparing the measured baseflow values with the simulated deep percolation values.

Measures were made weekly at least waiting, after precipitation events, for the watershed runoff time before taking the measurement. This allowed baseflow to be measured excluding runoff, which was calculated by continuous CN methodology. Of course, the presence of a permanent flow measurement station would have allowed for better calibration and validation, enabling water from runoff to be monitored as well.

Another innovative aspect, and useful in achieving better performance, is the use of an acclivity coefficient to consider the actual land area when calculating the parameter values of precipitation and potential evapotranspiration, which otherwise would have been respectively overestimated or underestimated.

Given the lack of detailed data on the territory (climate, soil, etc.), we decided to create a lumped-type model of water balance of the soil, where the value of each parameter is the weighted sum of all values that the parameter assumes in the watershed. This type of model has the disadvantage of providing less information about the spatial distribution of soil water balance parameter values (especially deep percolation, the unknown calculated in the balance), information that can be useful for localised studies and applications. In any case, the aim to spatialize at least qualitatively the deep percolation values of the model was solved by creating a map of infiltration propensity, intersecting through GIS the layers of predisposing factors (supplementary material 7 ). In fact, infiltration is closely related to deep percolation, although the two parameters are different.

Difficulties also arose because no crop coefficients ( $K_c$ ) specific to the study area were available while the model would need specific coefficients to perform better. Garofalo et al. (2011) pointed out that it is important to “calibrate”  $K_c$  for cultivars and soil and climate conditions in the growing environment, as they often differ from what is reported in FAO Paper No. 56. This can be achieved by making direct measurements of  $ET_c$  using weighing lysimeters, but this procedure is not always readily applicable, particularly for non-agricultural land uses such as uncultivated land, woods, or for orchards, vineyards, etc.

Here since direct measurements with weighing lysimeters were not possible, FAO coefficients were used, also as a basis for estimating coefficients for non-agricultural land uses. A crucial aspect of the study was indeed the determination of  $K_c$  for non-agricultural areas. FAO Paper No. 56 (chapter 9) provides equations for calculating  $K_c$  in vegetated areas. Corbari et al. (2017) used evapotranspiration measurements acquired from micrometeorological stations or through remote sensing to define the crop coefficients of vegetated natural areas, including deciduous forests, finding lower crop coefficient values than the FAO data, even though in climates other than Mediterranean. In our study the  $K_c$  values of uncultivated land and sparse and dense deciduous woods were calculated by means of a weighted sum of the  $K_c$  values of the land-use components (tab. 2.2 and 2.3), whose values are either reported in the FAO Paper or calculated from equations in the FAO Paper (which

consider local weather conditions). Given their important spatial extent in some areas, and the weight they have in the calculation of the unique watershed coefficient, the  $K_c$  of types of woods, more or less dense, should be carefully evaluated in future studies.

Another possibility for deriving crop coefficients specific to the study area is the use of the relationships between the Normalized Difference Vegetation Index (NDVI) and crop coefficients, as used by the spatially distributed SPHY model (Hunink et al., 2017). The same Authors conclude that for hydrological model applications at basin and sub-basin scale crop coefficient parameterization using satellite-based NDVI data is preferable, given the fact that sufficient long term series of NDVI data are now available for seasonal analyses at high resolution, and using literature-based crop coefficients can lead to wrong (generally under-estimated) streamflow simulations.

Considering the results, the lack of coefficient specificity and the use of FAO crop coefficients for the entire watershed does not appear to have had a significant impact on the performance of the phenological soil water balance model. Furthermore although not specific to the study area, the FAO coefficients are still reliable as demonstrated by Pereira et al. (2021), who updated the coefficients for some crop categories and found a good agreement with the  $K_c$  of FAO paper no. 56., In any case more studies should be done to evaluate these components.

The phenological soil water balance equation (eq. 9) allows calculation of the (daily, monthly, annual) unique value of deep percolation for the watershed. The most useful values of deep percolation provided by the model are not the single daily/monthly/annual totals (given the temporal discrepancy between deep percolation values and baseflow values) but the multi-annual totals or the multi-annual average value, which are really close to the true respective values of baseflow.

Future developments may improve the model by making it a distributed or semi-distributed type (for which, however, a larger amount of data would be needed) and implemented by means of a specific software. An example of software that utilises  $K_c$  (with the dual crop coefficient approach) for use in irrigation planning and scheduling and hydrologic water balances is SIM-dualKc (Rosa et al., 2011, Rosa et al., 2012); a software that calculates the phenological soil water balance would have the entire watershed as its reference area. Waiting for this possible future development, a strength of the current model is that only a spreadsheet and a GIS are needed to implement it.

The model can then be improved by searching for crop coefficients specific to the study area and calibrated in watersheds with continuous flow measurements. Fur-

thermore, up-to-date land use maps would be needed for good performance because the area extent of crop types varies from year to year. This can be obviated by considering these extents constant: the model would be less accurate but still reliable.

## 5. CONCLUSIONS

The need for adequate tools for evaluating the water resources of a watershed, and to understand hydrological dynamics at a deeper level, has led to the elaboration of a hydrological model to expand and improve the performance of the hydrological model proposed in FAO Paper No. 56. This model, here defined as a 'phenological soil water balance model', has innovative characteristics that enable the achievement of high levels of precision and accuracy. Firstly, it adopts a correction of the reference precipitation and evapotranspiration values, taking into account the actual area of the territory. It also applies to the whole watershed (therefore both for agricultural and non-agricultural land uses) the crop coefficients for the estimation of the maximum crop evapotranspiration, which are a function of the phenological stage. For this purpose it was necessary to research and compute crop coefficients for non-agricultural land use classes; a single daily coefficient, which is the weighted sum of the daily crop coefficients of all land use classes, was thus developed to correct the watershed potential evapotranspiration.

The model, applied for seven consecutive years (2013–2019), is lumped, physically based, deterministic and uses daily time intervals; it was calibrated and validated on a small watershed with low anthropic impact. The balance equation (Eq. 9) is valid at all time intervals (daily, weekly, monthly, annual, multi-annual). Calibration and validation were carried out by comparing the values of the deep percolation from the model with the measured baseflow at the closure section of the watershed. The consistency between the two values, which had an excellent correlation both as the trend and as multi-annual totals, demonstrated the validity of the model. Anyway further research that may lead to the determination of more suitable crop coefficients for the area under study, up-to-date land use maps, greater availability of climatic data for correcting the coefficients, making the model distributed and implementation through specific software may further improve the performance of the model.

The phenological soil water balance, which provides insights into surface and groundwater flows, allows for quantification, at different time intervals, of the potential surface and underground water resources and the water deficit for the entire watershed.

It can be a valuable technical-scientific aid for policymakers for proper water resources management, for planning the agricultural use of the watershed and also for the identification of the most suitable sites for building water collection reservoirs.

#### ACKNOWLEDGEMENTS

We would like to thank Drs. Piero Paolucci and Silvio Cecchini of 'A. Serpieri' meteorological observatory in Urbino for the data provided.

#### REFERENCES

- Allen R.G., Pereira L.S., Raes D., Smith M., 1998. Crop evapotranspiration: guidelines for computing crop water requirements. In: FAO Irrigation and Drainage Paper No. 56. FAO, Rome, Italy, pp 300.
- AA.VV., 2006. Suoli e Paesaggi delle Marche. ASSAM (Agency for Agro-food Sector Services of the Marche Region), Errebi Grafiche Ripesi, Falconara Marittima (Ancona, Italy), pp. 304.
- Barrera Jr. W.B., Ferrise R., Dalla Marta A. (2023) Understanding trends and gaps in global research of crop evapotranspiration: a bibliometric and thematic review. *Italian Journal of Agrometeorology* (1): 13-35. <https://doi.org/10.36253/ijam-2175>
- Becker A., Pfützner B., 1986. Identification and modelling of river flow reductions caused by evapotranspiration losses from shallow groundwater areas. 2nd Scientific Assembly of the IAHS, Symp. 52, Budapest, July 1986. IAHS Publ. No. 156, pp. 301–311.
- Brirhet H., Benaabidate L., 2016. Comparison of two hydrological models (lumped and distributed) over a pilot area of the Issen watershed in the Souss Basin, Morocco. *Eur. Sci. J.* 12(18): 347-358. <https://doi.org/10.19044/esj.2016.v12n18p347>.
- Budyko M.I., 1974. *Climate and Life*. Academic Press, New York, 508 pp.
- Corbari C., Ravazzani G., Galvagno M., Cremonese E., Mancini M., 2017. Assessing Crop Coefficients for Natural Vegetated Areas Using Satellite Data and Eddy Covariance Stations. *Sensors* (Basel). Nov 18;17(11): 2664. <https://doi.org/10.3390/s17112664>. PMID: 29156568; PMCID: PMC5713072.
- Costello L.R., Jones K.S., 2014. WUCOLS IV: Water Use Classification of Landscape Species. California Center for Urban Horticulture, University of California, Davis. <http://ucanr.edu/sites/WUCOLS/>
- Dripps W.R., Bradbury K.R., 2007. A simple daily soil-water balance model for estimating the spatial and temporal distribution of groundwater recharge in temperate humid areas. *Hydrogeol. J.* 15: 433–444. <https://doi.org/10.1007/s10040-007-0160-6>.
- Eccel E., Toller G., Ghielmi L., Salvadori C., La Porta N., 2007. Valutazione del bilancio idrico in una foresta decidua alpina. *Ital. J. Agrometeorol.* 12(1): 32-43.
- Farmer W.H., Vogel R.M., 2016. On the deterministic and stochastic use of hydrologic models, *Water Resour. Res.*, 52: 5619-5633. <https://doi.org/10.1002/2016WR019129>.
- Friuli-Venezia Giulia Autonomous Region, 2018. Piano regionale di tutela delle acque. <http://www.regione.fvg.it/rafvfg/cms/RAFVG/ambiente-territorio/pianificazione-gestione-territorio/FOGLIA20/FOGLIA22/>
- Garofalo P., Vonella A.V., Maddaluno C., Rinaldi M., 2011. Verifica dei coefficienti colturali (kc) su colture erbacee in una pianura del Sud Italia. Proc. of the XIV National Congress of Agrometeorology "Agrometeorologia per l'azienda agraria". 7-9 June 2011, Facoltà di Agraria, Bologna, 15-16.
- Gayathri K. Devi, Ganasri B.P., Dwarakish G.S., 2015. A review on hydrological models. *Aquat. Procedia*, 4: 1001–1007. <https://doi.org/10.1016/j.aqpro.2015.02.126>
- Garavaglia F., Le Lay M., Gottardi F., Garçon R., Gailhard J., Paquet E., Mathevet T., 2017. Impact of model structure on flow simulation and hydrological realism: from a lumped to a semi-distributed approach, *Hydrol. Earth Syst. Sci.*, 21: 3937–3952, <https://doi.org/10.5194/hess-21-3937-2017>
- Gori S., 2004. Valutazione della pericolosità di frana attraverso l'analisi di foto aeree e in relazione alle condizioni di innesco in un'area nel comune di Urbino. Degree Diss., Università di Urbino, Italy.
- Gupta H. V., Kling H., Yilmaz K. K., Martinez G. F., 2009. Decomposition of the mean squared error and NSE performance criteria: Implications for improving hydrological modelling. *J. Hydrol.*, 377(1-2): 80–91, doi:10.1016/j.jhydrol.2009.08.003
- Hunink J.E., Eekhout J.P.C., De Vente J., Contreras S., Droogers P., Baille A., 2017. Hydrological Modelling Using Satellite-Based Crop Coefficients: A Comparison of Methods at the Basin Scale. *Remote Sens.* 9(2): 174. <https://doi.org/10.3390/rs9020174>
- Jiménez Cisneros B.E., Oki T., Arnell N.W., Benito G., Cogley J.G., Döll P., Jiang T., Mwakalila S.S., 2014. Freshwater resources. In: *Climate Change 2014: Impacts, Adaptation, and Vulnerability. Part A: Global and Sectoral Aspects. Contribution of Working Group II to the Fifth Assessment Report of the Intergovernmental Panel on Climate Change* [Field, C.B., V.R. Barros, D.J. Dokken, K.J. Mach, M.D. Mastrandrea, T.E. Bilir, M. Chatterjee, K.L. Ebi, Y.O. Estrada, R.C. Genova, B. Girma, E.S. Kissel, A.N. Levy, S. MacCracken, P.R. Mastrandrea, and L.L. White (eds.)].

- Cambridge University Press, Cambridge, United Kingdom and New York, NY, USA, pp. 229-269.
- Kannan N., Santhi C., Williams J.R., Arnold J.G., 2008. Development of a continuous soil moisture accounting procedure for curve number methodology and its behaviour with different evapotranspiration methods. *Hydrol. Process.* 22(13): 2114-2121. <https://doi.org/10.1002/hyp.6811>.
- Khakbaz B., Imam B., Hsu K., Sorooshian S., 2012. From lumped to distributed via semi-distributed: Calibration strategies for semi-distributed hydrologic models. *Journal of Hydrology*, 418-419: 61-77. <https://doi.org/10.1016/j.jhydrol.2009.02.021>
- Knoben W.J.M., Freer J.E., Woods R.A., 2019. Technical note: Inherent benchmark or not? Comparing NashSutcliffe and Kling-Gupta efficiency scores. *Hydrology and Earth System Sciences*. <https://doi.org/10.5194/hess-2019-327>
- Mishra S.K., Singh V.P., 2003. Soil Conservation Service Curve Number (SCS-CN) Methodology. *Water Sci. Technol. Library*, vol 42. Springer, Dordrecht, The Netherlands, pp. 516. <https://doi.org/10.1007/978-94-017-0147-1>
- Mockus V., 1972. Chapter 10: Estimation of Direct Runoff from Storm Rainfall. US Department of Agriculture (Ed.), *Hydraulics and Hydrology — Technical References NRCS National Engineering Handbook*, Part 630 Hydrology, Washington DC.
- Neitsch S.L., Arnold J.G., Kiniry J.R., Williams J.R., 2011. Soil and Water Assessment Tool Theoretical documentation version 2009. Texas Water Resources Institute Technical Report No. 406, Texas A&M University System College Station, Texas 77843-2118
- Pereira L.S., Paredes P., Hunsaker D.J., López-Urrea R., Mohammadi Shad Z., 2021. Standard single and basal crop coefficients for field crops. Updates and advances to the FAO56 crop water requirements method. *Agricultural Water Management*, Volume 243: 106466. <https://doi.org/10.1016/j.agwat.2020.106466>.
- Rosa, R.D., Paredes, P., 2011. The SIMdualKc model. Software application for water balance computation and irrigation scheduling using the dual crop coefficient approach. CEER-Biosystems Engineering. Institute of Agronomy, Technical University of Lisbon.
- Rosa, R.D., Paredes, P., Rodrigues, G.C., Alves, I., Fernando, R.M., Pereira, L.S., Allen, R.G., 2012. Implementing the dual crop coefficient approach in interactive software. 1. Background and computational strategy. *Agricultural Water Management*. <https://doi.org/10.1016/j.agwat.2011.10.013>
- Schewe J., Heinke J., Gerten D., Haddeland I., Arnell N.W., Clark D.B., Dankers R., Eisner S., Fekete B., Colón-González F.J., Gosling S.N., Kim H., Liu X., Masaki Y., Portmann F.T., Satoh Y., Stacke T., Tang Q., Wada Y., Wisser D., Albrecht T., Frieler K., Piontek F., Warszawski L., Kabat P., 2013. Multi-model assessment of water scarcity under climate change. *Proceedings of the National Academy of Sciences of the United States of America* 111(9): 3245-3250. <https://doi.org/10.1073/pnas.1222460110>
- Schumann A.H., 1993. Development of conceptual semi-distributed hydrological models and estimation of their parameters with the aid of GIS. *Hydrol. Sci. J.* 38(6): 519-528. <https://doi.org/10.1080/02626669309492702>.
- Taurino L., 2004. Un sistema informativo territoriale per l'analisi della propensione al dissesto dei versanti dell'area urbinata. Degree Diss., Università di Urbino, Italy.
- UNI EN ISO 748:2008 – Misurazione della portata di liquidi in canali aperti mediante correntometri o galleggianti. International Standards Organization (ISO), Geneva, Switzerland, 2008.
- U.S. Army Corps of Engineers, 2013. Hydrologic modeling system HEC-HMS - User's Manual. Davis, CA, pp. 442. <http://www.hec.usace.army.mil/software/hec-hms/>.
- USDA NRCS, 2004. Part 630 – Hydrology National Engineering Handbook Natural Resources Conservation Service, Washington, D.C. <https://directives.sc.egov.usda.gov/viewerFS.aspx?hid=21422>
- Williams J.R., Arnold J.G., Srinivasan R., 2000. The APEX Model. BRC Report No. 00-06. Temple, TX: Texas A&M University, Texas Agricultural Extension Service, Texas Agricultural Experiment Station, Blacklands Research Center.
- Williams J.R., Izaurralde R.C., 2005. The APEX model. BREC Report No. 2005-02. Temple, Tex.: Texas A&M University, Texas Agricultural Experiment Station, Blackland Research and Extension Center.
- Williams J.R., Kannan N., Wang X., Santhi C., Arnold J.G., 2012. Evolution of the SCS Runoff Curve Number and its application to continuous runoff simulation. *J. Hydrol. Eng.* 17(11): 1221-1229. [https://doi.org/10.1061/\(ASCE\)HE.1943-5584.0000694](https://doi.org/10.1061/(ASCE)HE.1943-5584.0000694)
- Zotarelli L., Dukes M.D., Romero C.C., Migliaccio K.W., Morgan K.T., 2010. Step by Step Calculation of the Penman-Monteith Evapotranspiration (FAO-56 Method). Doc. AE459, University of Florida. <https://edis.ifas.ufl.edu/pdffiles/AE/AE45900.pdf>

SUPPLEMENTARY MATERIAL 1  
INSIGHT INTO THE CONCEPT OF THE COEFFICIENT  
OF ACCLIVITY AND ITS IMPLICATIONS IN THE  
PHENOLOGICAL SOIL WATER BALANCE

When calculating how much water has rained in a territory, the surface of the territory is considered as if it were flat (fig. S1/A); i.e. on the projected surface.

However, a correction should be made to distribute the precipitation over the actual surface. If it is assumed that, above the watershed line, the watershed is 'covered' by a flat surface, the precipitation water is distributed over this, which corresponds to the projected surface of

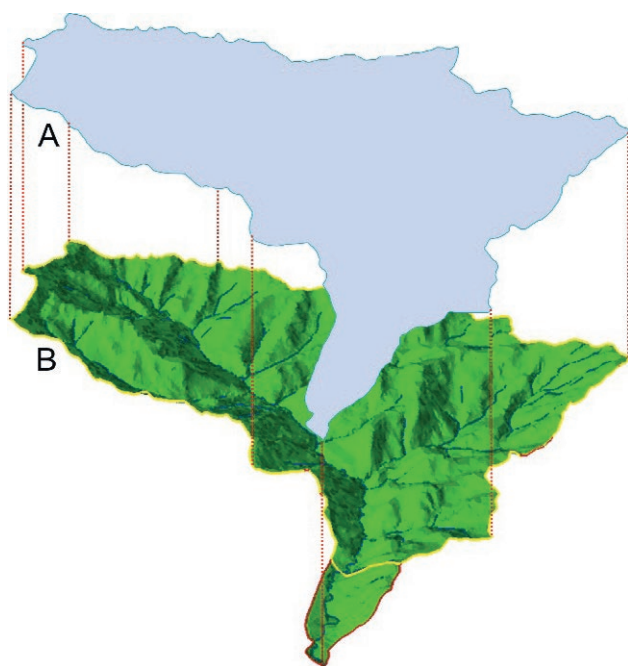


Figure S1/A. Projected surface of Santa Maria degli Angeli watershed.

Figure S1/B. Actual surface of Santa Maria degli Angeli watershed.

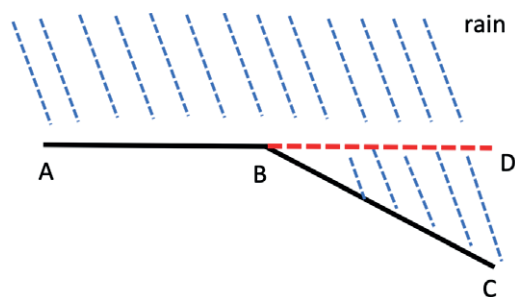


Figure S2. Schematisation of conditions for the application of the acclivity coefficient ( $C_a$ ).

the basin (fig. S1/A): for the Santa Maria degli Angeli watershed the area of this surface is 13.098 km<sup>2</sup>.

However, the water is not distributed over this theoretical surface but is distributed over a larger, effective one (fig. S1/B), that for Maria degli Angeli watershed has an area of 13.979 km<sup>2</sup>. The values indicated relate to the portion of watershed on which the balance was calculated, highlighted by the yellow line in figure S1/B.

The measure of the projected area was calculated using GIS, the measure of the actual area was calculated using a Digital Terrain Model.

Fig. S2 schematises this process in 2 dimensions. The broken line ABC is the ground profile. The segment BD corresponds to the projected surface of BC; we have that  $AB=BD$ , and obviously  $BC>AB$  and  $BC>BD$ .

The amount of water that falls on AB and BD is the same, but the amount that falls on BD is distributed over a larger surface, i.e. BC, resulting in a decrease in the precipitation value per unit of soil. For evapotranspiration, the effect is the opposite: the actual evapotranspirative surface is greater than the projected surface, so the losses per ET are greater. This effect is greater the greater the slope angle.

SUPPLEMENTARY MATERIAL 2

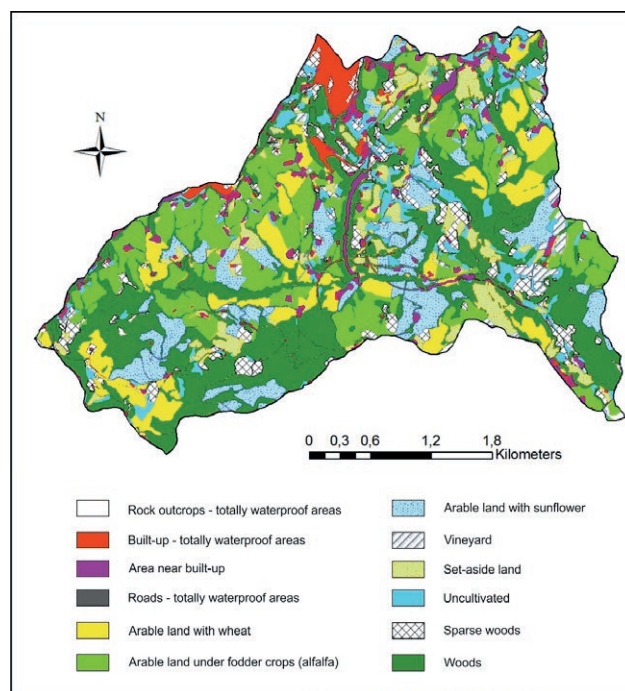
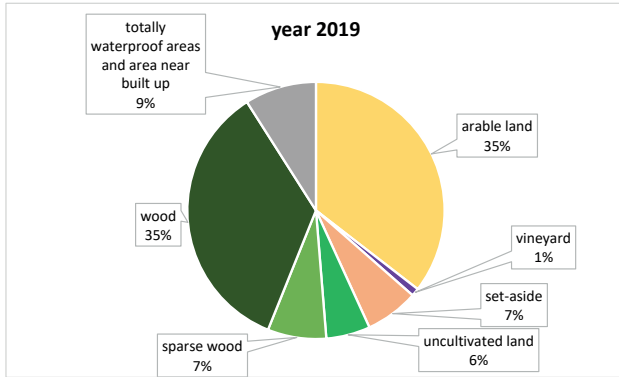


Figure S3. Land use map of Santa Maria degli Angeli watershed for the year 2013, obtained by interpretation of aerial orthophotos and processed on vector files in a GIS environment. The 'area near built-up' land use includes mixed built-up and natural areas with low anthropogenic impact.



**Figure S4.** Percentage distribution of land use classes in the Santa Maria degli Angeli watershed, year 2019.

### SUPPLEMENTARY MATERIAL 3 CALCULATION OF RUNOFF

For the calculation of the daily values of the runoff parameter, which contribute to the phenological soil water balance (see Eq. 1), the curve number methodology (Mockus, 1972; USDA, 2004), with its subsequent modifications (Williams, 2000; Kannan et al., 2008; Friuli Venezia Giulia Autonomous Region, 2018), was used.

#### S3.1. USDA Curve Number method

Each territory was assigned a parameter called Curve Number (CN), which has a value between 0 and 100. Each value of CN corresponds to a curve through which, based on the precipitation value, the percentage of runoff is obtained. Higher CN values correspond to higher runoff values.

The CN value of a watershed is a function of:

- land use;
- permeability of soils;
- average slope of the watershed; and
- antecedent soil moisture conditions (AMC).

**Table S.1.** Cumulative precipitation intervals (in mm) for each of the vegetative phases considered and corresponding classes of antecedent soil moisture conditions (AMC) and curve number (CN). The values reported in the dormancy, growing and average columns are cumulative precipitation of the 5 days before the day in which the runoff was calculated.

Dormancy	Average	Growing	AMC class	CN class
<13	<23	<36	I	CN I
13-28	23-40	36-53	II	CN II
>28	>40	>53	III	CN III

Precipitation water is initially retained by leaf interception, ground depressions and infiltration: this quantity is called ‘initial abstraction’ (Ia) and the runoff begins only after Ia has been saturated.

Each soil has a maximum water storage value corresponding to the potential maximum retention (S, expressed in mm). This parameter is related to the CN according to the following two equations:

$$CN = \frac{25400}{254 + S} \quad (1S)$$

$$S = \frac{25400}{CN} - 254 \quad (2S)$$

The share of water that must provide the rain to saturate the initial abstraction is equal to:

$$Ia = 0.2 \cdot S \quad (3S)$$

The value of 0.2 may vary depending on the site and other parameters but is considered to be reliable in many cases.

For a given precipitation amount, the amount of runoff (RO<sup>7</sup>, mm) is as follows (USDA NRCS, 2004):

$$RO = 0 \quad \text{if } P \leq Ia$$

$$RO = \frac{(P - Ia)^2}{P - Ia + S} \quad \text{if } P > Ia \quad (4S)$$

The parameter S has a constant value depending on the CN of the territory and this implies that, even if the soils had a different degree of humidity, the share of runoff would still be the same with equal precipitation. To overcome this limit, the parameter AMC (antecedent soil moisture condition) was introduced; it is a function of the vegetative phase and the cumulative rainfall of the 5 days before the day for which the runoff is to be calculated and determines which CN value is to be used. Table S.1 shows the threshold values for each AMC and the corresponding CN.

#### S3.2. USDA Curve Number method using a continuous soil moisture accounting procedure: application to the case study

The ranges of cumulative rainfall values over the previous 5 days for each AMC class in the study area

<sup>7</sup> Note: in the original formula of the CN the runoff is indicated with the abbreviation ‘Q’. To avoid confusion, the abbreviation ‘RO’ given in FAO Paper No. 56 and in the phenological soil water balance equation (Eq. 1) has also been used here.

**Table S.2.** Ranges for antecedent soil moisture conditions (AMC) for the Santa Maria degli Angeli watershed in the year 2019, corresponding to cumulative precipitation (mm) in the previous 5 days.

AMC classes		Jan	Feb	Mar	Apr	May	Jun	Jul	Aug	Sept	Oct	Nov	Dec
AMC I	<	12	12	17	22	30	32	30	31	26	22	17	12
AMC II	between	12-26	12-26	17-32	22-38	30-46	32-48	30-46	31-47	26-39	22-38	17-32	12-26
AMC III	>	26	26	32	38	46	48	46	47	39	38	32	26

**Table S.3.** Correspondence between USDA classes and land use classes of the Santa Maria degli Angeli watershed for the calculation of CN.

USDA class [CN values associated with the 4 soil groups]	land use class of the S.M.A. watershed
Paved parking lots, paved streets and roads [98, 98, 98, 98]	Impermeable soil
Urban districts: commercial and business (imp. 85%) [89, 92, 94, 95]	Built-up
Residential districts (imp. 65%) [77, 85, 90, 92]	Area near built-up
Small grain – contoured – good conditions [61, 73, 81, 84]	Arable land winter wheat
Row crops – contoured+crop residue cover – good conditions [64, 74, 81, 85]	Arable land sunflower
Close-seeded or broadcast legumes or rotation meadow – contoured – good conditions [55, 69, 78, 83]	Arable land alfalfa, faba bean, clover
Pasture, grassland, or range-continuous forage for grazing – good conditions [39, 61, 74, 80]	Set aside
Brush-brush-forbs-grass mixture with brush the major element – fair conditions [35, 56, 70, 77]	Uncultivated
Woods-grass combination – good conditions [32, 58, 72, 79]	sparse wood
Woods – good conditions [30, 55, 70, 77]	wood

were calculated monthly based on the vegetative phases of the components of the entire watershed land use classes. By way of example, the values for the year 2019 are given in Table S.2. Values should be recalculated if the areas of the land use class components vary.

In this study, AMC ranges were used for the calculation of parameter B of the equation 6S (Williams et al., 2000).

The procedure for determining the CN value of the watershed is reported in the Hydrology National Engineering Handbook (USDA NRCS, 2004). For this purpose, it was necessary to attribute the land use classes present in the watershed to the land use classes provided for by the method (Table S.3).

From the weighted sum of the values of the curve numbers of all uses of the soil the value of CN for the entire watershed is obtained. This value shall be corrected for the mean slope of the watershed. This is achieved by substituting, in equation 1S, the parameter S with  $S_{2s}$  (maximum soil water retention), calculated by equation 5S (Williams and Izaurralde, 2005; Williams et al., 2012).

$$S_{2s} = S_2 \cdot \left[ 1.1 - \frac{STP}{STP + \exp(3.7 + 0.02117 \cdot STP)} \right] \quad (5S)$$

where:

STP: average slope of the watershed (%); and

$S_2$ : S value derived from equation 2S using the  $CN_2$  value found.

The corrected value of CN is expressed by the abbreviation  $CN_{2s}$ .

To calculate the actual daily runoff it is necessary to replace, in equation 4S, the value of S with the daily value of retention ( $S_t$ ). This value is obtained with the following equation (Williams et al., 2000; Kannan et al., 2008).

$$S_t = S_{t-1} + ET_{0t} \cdot \exp\left(\frac{-B \cdot S_{t-1}}{S_{max}}\right) - P_{t-1} + Q_{t-1} \quad (6S)$$

where:

$S_t$ : retention parameter of the day  $t$

$ET_{0t}$ : potential evapotranspiration of day  $t$  (the  $ET_c$  was used)

$S_{t-1}$ : retention parameter of the day  $t-1$

B: depletion parameter.<sup>8</sup>

$P_{t-1}$ : precipitation of the previous day ( $P_a$  was used)

$Q_{t-1}$ : runoff of the previous day

<sup>8</sup> The value should theoretically be between 0 and 2, in practice it fluctuates between 0.5 and 1.5. In this study, the following values were assigned to B according to soil moisture conditions: with AMC I B = 0,75, with AMC II B = 1, with AMC III B = 1,25

$S_{max}$ : maximum value of the retention parameter, corresponding to the value of  $S$  obtained by placing in equation 2S the value of  $CN_1$ .

For the first of the balance years, in the absence of data relating to previous periods, the starting value of  $S_t$  when  $t = 0$  is obtained by placing the value of  $CN_{2s}$  in equation 2S. For subsequent years, the starting value of  $S_t$  is that of the last day of the previous year.

The parameter  $S_t$  has an upper limit,  $S_{max}$ , which is obtained by placing the value of  $CN_1$  instead of  $CN$  in equation 2S. For the calculation of  $CN_1$ , equation 7S is used (Williams and Izaurralde, 2005; Williams et al., 2012).

$$CN_1 = CN_{2s} - \frac{20 \cdot (100 - CN_{2s})}{100 - CN_{2s} + \exp[2.533 - 0.0636 \cdot (100 - CN_{2s})]} \quad (7S)$$

If the parameter  $S$  assumed the value of 0 in equation 1S,  $CN$  would assume the value of 100, which is a characteristic value of completely impermeable surfaces; this would lead to overestimation of the runoff. Consequently, following the methodology used for the realisation of the Regional Plan for the Protection of Waters of the Friuli Venezia Giulia Autonomous Region (2018), a lower limit,  $S_{min}$ , has also been established, which is obtained by placing the value of  $CN_3$  in equation 2S.

**Table S.4.** Values of the  $CN_2$  and the various types of  $CN$  in the 7 years in which the phenological soil water balance was elaborated.

Year	$CN_2$ Value	CN Class	Value
2013	73,9	$CN_1$	60,2
		$CN_{2s}$	77,8
		$CN_3$	90,3
2014	74,1	$CN_1$	60,3
		$CN_{2s}$	77,9
		$CN_3$	90,4
2015	73,9	$CN_1$	60,1
		$CN_{2s}$	77,7
		$CN_3$	90,3
2016	73,8	$CN_1$	60,0
		$CN_{2s}$	77,6
		$CN_3$	90,2
2017	73,6	$CN_1$	59,8
		$CN_{2s}$	77,4
		$CN_3$	90,1
2018	73,5	$CN_1$	59,7
		$CN_{2s}$	77,4
		$CN_3$	90,1
2019	73,7	$CN_1$	59,9
		$CN_{2s}$	77,5
		$CN_3$	90,2

For the calculation of  $CN_3$ , equation 8S is used (Williams and Izaurralde, 2005; Williams et al., 2012).

$$CN_3 = CN_{2s} \exp [0.00673 \cdot (100 - CN_{2s})] \quad (8S)$$

The values of the three classes of  $CN$  corrected for the slope in the seven years in which the phenological soil water balance was developed are reported in Table S.4.

### S3.3 Calculation of runoff: step-by-step procedure and an example of calculation of runoff in selected periods of the year 2015

The following are the steps for the calculation of runoff (the symbols are those already described in the text):

- 1) calculation of the values  $S_{t=0}$ ,  $S_{max}$  and  $S_{min}$  (insertion in eq. 2S of the values of  $CN_{2s}$ ,  $CN_1$  and  $CN_3$ );
- 2) for each simulation day the values of the basic parameters  $P_a$ ,  $ET_c$ ,  $B$  are to be entered;
- 3) for each day,  $S_t$  is to be calculated using equation 6S; the starting value in the first balance year is  $S_{t=0}$ , in the following years the starting value is  $S_t$  of the last day of the previous year;
- 4) initial abstraction ( $= 0,2 \cdot S_t$ ) is to be calculated for each day;
- 5) the runoff (RO) is to be calculated for each day according to equation 4S;
- 6) If  $S_t < S_{min}$ , it poses  $S_t = S_{min}$ ; and
- 7) If  $S_t > S_{max}$ , it poses  $S_t = S_{max}$ .

Below are reported some examples of the calculation of runoff in characteristic periods of the year 2015, in which  $S_{max} = 168,48$  and  $S_{min} = 27,32$ .

#### First period: winter phase

For 21–22 January, it was noted that there was moderate precipitation and no runoff (RO); this was determined as  $P-Ia \leq 0$ ; in fact, there can be no runoff until the initial abstraction is not completely compensated. On January 23, the runoff (RO) started, as  $P-Ia > 0$  and, simultaneously,  $S_t$  decreased below the value of  $S_{min}$ ; in this case, the value of  $S_t$  must be replaced with  $S_{min}$ .

#### Second period: spring phase

In this period  $S_t$  assumes intermediate values between  $S_{min}$  and  $S_{max}$ , and with precipitation of a certain consistency, there is runoff ( $RO > 0$ ). Note the drastic drop in  $S_t$  after a day of heavy precipitation and subsequent runoff. The value of  $S_t$ , however, also depends on  $ET_c$  and  $B$  (Eq. 6S).



**Table S.5.** Runoff calculation model - winter 2015.  $P_a$ : precipitation values corrected for acclivity coefficient;  $ET_c$ : evapotranspiration crop of the watershed; B: depletion parameter (varies between 0.75 and 1.25);  $S_t$ : day retention parameter t; Ia: initial abstraction; RO: runoff.

Date	$P_a$ (mm)	$ET_c$ (mm)	B	$S_t$ (mm)	Ia (mm)	$P_a$ -Ia (mm)	RO (mm)
21/01/2015	0.8	0.41	0.75	35.08	7.016	-6.2	0.0
22/01/2015	2.3	0.58	0.75	34.74	6.947	-4.7	0.0
23/01/2015	10.5	0.32	0.75	32.73	6.545	3.9	0.4
24/01/2015	2.2	0.70	1	27.32	5.464	-3.3	0.0
25/01/2015	0.2	1.21	1	27.32	5.464	-5.3	0.0
26/01/2015	0.0	0.98	1	27.96	5.593	-5.6	0.0
27/01/2015	0.0	0.76	1	28.61	5.721	-5.7	0.0
28/01/2015	0.0	0.83	1	29.30	5.861	-5.9	0.0
29/01/2015	1.4	1.78	0.75	30.87	6.174	-4.8	0.0
30/01/2015	7.7	1.89	0.75	31.11	6.222	1.5	0.1
31/01/2015	0.1	1.46	0.75	27.32	5.464	-5.3	0.0
01/02/2015	1.8	0.53	0.75	27.66	5.532	-3.8	0.0
02/02/2015	0.1	1.27	0.75	27.32	5.464	-5.4	0.0
03/02/2015	0.0	0.96	0.75	28.11	5.622	-5.6	0.0
04/02/2015	10.6	0.70	0.75	28.72	5.745	4.9	0.7
05/02/2015	29.2	0.44	1	27.32	5.464	23.8	11.1
06/02/2015	48.2	0.36	1.25	27.32	5.464	42.7	26.0
07/02/2015	7.7	0.43	1.25	27.32	5.464	2.3	0.2
08/02/2015	3.2	1.20	1.25	27.32	5.464	-2.3	0.0
09/02/2015	0.2	1.38	1.25	27.32	5.464	-5.2	0.0
10/02/2015	0.0	1.16	1.25	28.02	5.603	-5.6	0.0

**Table S.6.** Runoff calculation model - spring 2015. For explanation of symbols see table S5 legend.

Date	$P_a$ (mm)	$ET_c$ (mm)	B	$S_t$ (mm)	Ia (mm)	$P_a$ -Ia (mm)	RO (mm)
19/05/2015	0.0	6.08	0.75	96.385	19.277	-19.3	0.0
20/05/2015	0.0	4.83	0.75	99.529	19.906	-19.9	0.0
21/05/2015	0.0	4.96	0.75	102.711	20.542	-20.5	0.0
22/05/2015	66.5	1.13	0.75	103.424	20.685	45.8	14.0
23/05/2015	15.0	1.88	1.25	51.878	10.376	4.6	0.4
24/05/2015	6.2	2.16	1.25	38.760	7.752	-1.5	0.0
25/05/2015	0.1	3.95	1.25	35.476	7.095	-7.0	0.0
26/05/2015	1.6	3.31	1.25	37.960	7.592	-6.0	0.0
27/05/2015	15.9	2.34	1.25	38.168	7.634	8.3	1.5
28/05/2015	0.0	4.85	1	27.607	5.521	-5.5	0.0
29/05/2015	0.0	5.30	0.75	32.293	6.459	-6.5	0.0

Third period: summer phase

Precipitation is low and does not produce runoffs. The high values of  $ET_c$  raise  $S_t$  that exceeds  $S_{max}$ : in this

**Table S.7.** Runoff calculation model - summer 2015. For explanation of symbols see table S5 legend.

Date	$P_a$ (mm)	$ET_c$ (mm)	B	$S_t$ (mm)	Ia (mm)	$P_a$ -Ia (mm)	RO (mm)
15/07/2015	0.0	4.98	0.75	163.122	32.624	-32.6	0.0
16/07/2015	2.9	5.06	0.75	165.572	33.114	-30.2	0.0
17/07/2015	0.0	6.07	0.75	165.603	33.121	-33.1	0.0
18/07/2015	0.0	5.27	0.75	168.122	33.624	-33.6	0.0
19/07/2015	0.0	5.99	0.75	168.475	33.695	-33.7	0.0
20/07/2015	0.0	5.53	0.75	168.475	33.695	-33.7	0.0
21/07/2015	0.0	5.22	0.75	168.475	33.695	-33.7	0.0
22/07/2015	0.0	4.75	0.75	168.475	33.695	-33.7	0.0
23/07/2015	0.0	5.43	0.75	168.475	33.695	-33.7	0.0
24/07/2015	0.1	4.47	0.75	168.475	33.695	-33.6	0.0

**Table S.8.** Runoff calculation model - autumn 2015. For explanation of symbols see table S5 legend.

Date	$P_a$ (mm)	$ET_c$ (mm)	B	$S_t$ (mm)	Ia (mm)	$P_a$ -Ia (mm)	RO (mm)
21/09/2015	0.0	1.99	0.75	168.475	33.695	-33.7	0.0
22/09/2015	0.0	2.09	0.75	168.475	33.695	-33.7	0.0
23/09/2015	9.4	1.77	0.75	168.475	33.695	-24.3	0.0
24/09/2015	31.6	1.26	0.75	159.638	31.928	-0.3	0.0
25/09/2015	8.2	0.79	1.25	128.241	25.648	-17.5	0.0
26/09/2015	0.3	1.35	1.25	120.578	24.116	-23.8	0.0
27/09/2015	0.9	2.68	1.25	121.329	24.266	-23.4	0.0
17/11/2015	0.1	0.20	0.75	31.429	6.286	-6.2	0.0
18/11/2015	0.0	0.35	0.75	31.609	6.322	-6.3	0.0
19/11/2015	0.3	0.74	0.75	32.252	6.450	-6.2	0.0
20/11/2015	0.0	2.87	0.75	34.456	6.891	-6.9	0.0
21/11/2015	8.9	2.67	0.75	36.747	7.349	1.5	0.1
22/11/2015	19.6	0.55	0.75	28.405	5.681	13.9	4.6
23/11/2015	10.4	0.41	1	27.319	5.464	5.0	0.8
24/11/2015	0.0	0.44	1.25	27.319	5.464	-5.5	0.0
25/11/2015	0.4	0.42	1.25	27.658	5.532	-5.1	0.0
26/11/2015	3.9	0.87	1.25	27.930	5.586	-1.7	0.0
27/11/2015	7.9	0.80	1.25	27.319	5.464	2.4	0.2
28/11/2015	0.0	0.47	1	27.319	5.464	-5.5	0.0
29/11/2015	0.1	0.52	0.75	27.783	5.557	-5.5	0.0
30/11/2015	0.0	1.44	0.75	28.993	5.799	-5.8	0.0

case, the value of  $S_t$  is replaced with  $S_{max}$ , whose value cannot be exceeded.

Fourth and fifth period: autumn phase

The last two periods shall be reported together; in the fourth period the first substantial precipitation

events do not produce runoffs (since  $S_t$  has maximum value and initial abstraction is very high), but the  $S_t$  parameter begins to drop permanently. After a couple of months, it again reaches the value of  $S_{min}$  and fluctuates around this value until the end of the year. As a result, the runoff is quite consistent.

SUPPLEMENTARY MATERIAL 4  
MONTHLY VALUES OF THE DEEP PERCOLATION  
(SIMULATED BY THE PHENOLOGICAL SOIL WATER  
BALANCE) AND BASE FLOW OF THE SANTA MARIA  
DEGLI ANGELI STREAM (CALCULATED FROM  
DISCHARGE MEASUREMENTS) OVER THE PERIOD  
2013-2019

**Table S.9.**

Year	Month	Deep percolation (mm)	Measured baseflow (mm)	
2013	January	76,5	44,4	
	February	54,1	57,7	
	March	48,0	70,6	
	April	14,8	22,6	
	May	0,0	9,4	
	June	0,0	4,0	
	July	0,0	1,0	
	August	0,0	8,4	
	September	0,0	1,1	
	October	0,0	4,4	
	November	77,1	24,4	
	December	8,6	26,0	
2014	January	35,1	24,1	
	February	42,6	69,9	
	March	42,3	41,2	
	April	7,5	60,4	
	May	26,9	52,7	
	June	0,0	9,1	
	July	0,0	3,6	
	August	0,0	2,5	
	September	0,0	5,3	
	October	0,0	10,6	
	November	31,1	18,5	
	December	59,5	54,4	
2015	January	5,5	31,9	
	February	82,7	58,8	
	March	75,8	68,5	
	April	7,8	32,1	
	May	0,0	14,6	
	June	0,0	9,1	
	July	0,0	2,4	
	August	0,0	0,8	
	September	0,0	0,3	
	October	11,8	3,2	
	2016	November	29,6	4,0
		December	0,0	2,6
January		40,2	12,6	
February		41,8	19,9	
March		48,4	55,7	
April		0,0	13,7	
May		4,0	15,2	
June		0,0	5,1	
July		0,0	1,7	
August		0,0	1,1	
September		0,0	0,5	
October		0,0	0,5	
2017	November	6,7	3,4	
	December	0,0	1,2	
	January	47,6	23,2	
	February	33,5	24,0	
	March	14,9	29,6	
	April	0,0	8,7	
	May	0,0	4,5	
	June	0,0	0,2	
	July	0,0	0,8	
	August	0,0	0,9	
	September	0,0	0,9	
	October	0,0	0,1	
2018	November	23,5	1,2	
	December	37,4	10,2	
	January	1,6	11,3	
	February	122,5	52,5	
	March	83,5	125,5	
	April	0,0	21,8	
	May	0,0	9,2	
	June	0,0	2,2	
	July	0,0	1,6	
	August	0,0	0,8	
	September	0,0	0,4	
	October	0,0	0,0	
2019	November	9,0	1,6	
	December	34,6	7,8	
	January	34,5	9,0	
	February	10,9	16,9	
	March	0,0	5,3	
	April	0,0	5,0	
	May	34,6	30,1	
	June	0,0	25,1	
	July	0,0	2,2	
	August	0,0	1,1	
	September	0,0	0,3	
	October	0,0	2,5	
November	12,6	8,1		
December	20,8	14,4		
<i>Totals</i>		<i>1400</i>	<i>1444</i>	

## SUPPLEMENTARY MATERIAL 5

*The phenological soil water balance at significant periods during the year***Table S.10.** The phenological soil water balance in a phase of surplus during the year 2014 and determination of deep percolation.

Date	$ET_{0a} \cdot K_{c\ ws} = ET_c$		$ET_c \cdot K_s = aET_c$		$TAW \cdot p = RAW$			$P_a - RO - aET_c - \Delta AW = DP$							
	$ET_{0a}$	$K_{c\ ws}$	$ET_c$	$K_s$	TAW	p	RAW	$D_{r\ start}$	$D_{r\ end}$	AW	$P_a$	RO	$aET_c$	$\Delta AW$	DP
18/01/2014	1.97	1.05	2.06	1.00	129.5	0.688	89.1	5.56	7.62	121.9	0.0	0.0	2.1	-2.1	0.0
19/01/2014	1.54	1.05	1.61	1.00	129.5	0.688	89.1	7.62	7.79	121.7	1.4	0.0	1.6	-0.2	0.0
20/01/2014	0.89	1.05	0.93	1.00	129.5	0.688	89.1	7.79	8.22	121.3	0.5	0.0	0.9	-0.4	0.0
21/01/2014	0.40	1.05	0.42	1.00	129.5	0.688	89.1	8.22	<b>(-9.57)</b>	<b>129.5</b>	24.2	6.0	0.4	8.2	<b>9.6</b>
22/01/2014	0.80	1.05	0.83	1.00	129.5	0.688	89.1	<b>0.00</b>	0.71	128.8	0.1	0.0	0.8	-0.7	0.0
23/01/2014	0.85	1.05	0.89	1.00	129.5	0.688	89.1	0.71	0.50	129.0	1.1	0.0	0.9	0.2	0.0
24/01/2014	0.83	1.05	0.86	1.00	129.5	0.688	89.1	0.50	<b>(-10.44)</b>	<b>129.5</b>	13.7	1.9	0.9	0.5	<b>10.4</b>
25/01/2014	1.41	1.05	1.47	1.00	129.5	0.688	89.1	<b>0.00</b>	1.41	128.1	0.1	0.0	1.5	-1.4	0.0
26/01/2014	0.72	1.05	0.76	1.00	129.5	0.688	89.1	1.41	2.17	127.3	0.0	0.0	0.8	-0.8	0.0
27/01/2014	0.83	1.05	0.87	1.00	129.5	0.688	89.1	2.17	<b>(-0.24)</b>	<b>129.5</b>	3.3	0.0	0.9	2.2	<b>0.2</b>
28/01/2014	0.43	1.05	0.45	1.00	129.5	0.688	89.1	<b>0.00</b>	<b>(-1.52)</b>	<b>129.5</b>	2.0	0.0	0.5	0.0	<b>1.5</b>

$ET_{0a}$ : reference evapotranspiration corrected for acclivity coefficient (eq. 4 in the main article);

$K_{c\ ws}$ : unique 'crop' coefficient of the territory (eq. 6);

$ET_c$ : crop evapotranspiration of the territory (eq. 7);

TAW: total available water (see FAO paper 56, ch.8);

p: parameter for RAW calculation (see FAO paper 56, ch.8);

RAW: rapidly available water (see FAO paper 56, ch.8);

$D_{r\ start}$ : water deficit at the beginning of the day (=  $D_r$  end of the previous day)

$D_{r\ end}$ : water deficit at the end of the day (=  $D_r$  start +  $aET_c$  -  $P_a$  + RO). Note: the negative values of  $D_r$  end correspond to the positive values (in bold) of water surplus that go into deep percolation. So, the next day's  $D_r$  start value is zero;

$P_a$ : precipitation values corrected for acclivity coefficient (eq. 3);

RO: runoff (eq. 4S);

$K_s$ : water stress coefficient (see FAO paper 56, ch.8);

$aET_c$ : actual crop evapotranspiration (eq. 8);

AW: available water (= TAW -  $D_{r\ end}$ );

DP: deep percolation (eq. 9); and

$\Delta AW$ : variation of the available water with respect to the previous day.

Note: The phenological soil water balance is strictly represented by the parameters in the last 5 columns, and the equation that combines them together (shown at the top right of the table, that is the equation 9 in the main article). The other parameters are preliminary parameters to the balance.

**Table S.11.** The phenological soil water balance in conditions of a water stress period during the year 2014. For explanation of the symbols, see Table S10.

date	$ET_{0a} \cdot K_{c\ ws} = ET_c$		$ET_c \cdot K_s = aET_c$		$TAW \cdot p = RAW$			$P_a - RO - aET_c - \Delta AW = DP$							
	$ET_{0a}$	$K_{c\ ws}$	$ET_c$	$K_s$	TAW	p	RAW	$D_{r\ start}$	$D_{r\ end}$	AW	$P_a$	RO	$aET_c$	$\Delta AW$	DP
19/05/2014	3.72	1.00	3.74	1.00	129.5	0.547	70.8	53.15	56.89	72.6	0.0	0.0	3.7	-3.7	0.0
20/05/2014	4.48	1.01	4.50	1.00	129.5	0.547	70.8	56.89	61.39	68.1	0.0	0.0	4.5	-4.5	0.0
21/05/2014	5.54	1.01	5.58	1.00	129.5	0.547	70.8	61.39	66.97	62.5	0.0	0.0	5.6	-5.6	0.0
22/05/2014	6.00	1.01	6.04	1.00	129.5	0.547	70.8	66.97	73.01	56.5	0.0	0.0	6.0	-6.0	0.0
23/05/2014	3.50	1.01	3.52	0.96	129.5	0.547	70.8	73.01	76.41	53.1	0.0	0.0	3.4	-3.4	0.0
24/05/2014	6.25	1.01	6.29	0.91	129.5	0.547	70.8	76.41	82.10	47.4	0.0	0.0	5.7	-5.7	0.0
25/05/2014	4.31	1.01	4.34	0.81	129.5	0.547	70.8	82.10	85.42	44.1	0.2	0.0	3.5	-3.3	0.0

**Table S.12.** Available water to the seasonal lows during the 2015. For explanation of the symbols, see Table S.10.

date	$ET_{0a} \cdot K_{c\ w_s} = ET_c$		$ET_c \cdot K_s = aET_c$		$TAW \cdot p = RAW$			$P_a - RO - aET_c - \Delta AW = DP$							
	$ET_{0a}$	$K_{c\ w_s}$	$ET_c$	$K_s$	TAW	p	RAW	$D_{r\ start}$	$D_{r\ end}$	AW	$P_a$	RO	$aET_c$	$\Delta AW$	DP
02/08/2015	2.40	0.79	1.90	0.03	125.2	0.555	69.5	123.37	123.43	1.8	0.0	0.0	0.1	-0.1	0.0
03/08/2015	5.42	0.79	4.27	0.03	125.2	0.555	69.5	123.43	123.57	1.6	0.0	0.0	0.1	-0.1	0.0
04/08/2015	5.90	0.79	4.65	0.03	125.2	0.555	69.5	123.57	123.70	1.5	0.0	0.0	0.1	-0.1	0.0
05/08/2015	5.97	0.79	4.71	0.03	125.2	0.555	69.5	123.70	123.83	1.4	0.0	0.0	0.1	-0.1	0.0
06/08/2015	6.07	0.79	4.79	0.02	125.2	0.555	69.5	123.83	123.95	1.3	0.0	0.0	0.1	-0.1	0.0
07/08/2015	5.87	0.79	4.62	0.02	125.2	0.555	69.5	123.95	124.05	1.1	0.0	0.0	0.1	-0.1	0.0
08/08/2015	5.82	0.79	4.58	0.02	125.2	0.555	69.5	124.05	124.14	1.0	0.0	0.0	0.1	-0.1	0.0
09/08/2015	5.40	0.79	4.25	0.02	125.2	0.555	69.5	124.14	117.79	7.4	6.4	0.0	0.1	6.3	0.0
10/08/2015	3.75	0.79	2.95	0.13	125.2	0.555	69.5	117.79	113.90	11.3	4.3	0.0	0.4	3.9	0.0
11/08/2015	4.56	0.79	3.59	0.20	125.2	0.555	69.5	113.90	113.88	11.3	0.7	0.0	0.7	0.0	0.0
12/08/2015	5.61	0.79	4.41	0.20	125.2	0.555	69.5	113.88	114.78	10.4	0.0	0.0	0.9	-0.9	0.0

**Table S.13.** A period of the 2016 phenological soil water balance with fluctuations of the available water around the lows in the summer months. For explanation of the symbols, see Table S.10.

date	$ET_{0a} \cdot K_{c\ w_s} = ET_c$		$ET_c \cdot K_s = aET_c$		$TAW \cdot p = RAW$			$P_a - RO - aET_c - \Delta AW = DP$							
	$ET_{0a}$	$K_{c\ w_s}$	$ET_c$	$K_s$	TAW	p	RAW	$D_{r\ start}$	$D_{r\ end}$	AW	$P_a$	RO	$aET_c$	$\Delta AW$	DP
04/07/2016	5.41	0.85	4.59	0.23	129.3	0.539	69.7	115.30	116.38	12.9	0.0	0.0	1.1	-1.1	0.0
05/07/2016	6.20	0.84	5.20	0.22	129.3	0.539	69.7	116.38	117.50	11.8	0.0	0.0	1.1	-1.1	0.0
06/07/2016	4.60	0.83	3.81	0.20	129.3	0.539	69.7	117.50	116.60	12.7	1.7	0.0	0.8	0.9	0.0
07/07/2016	6.08	0.82	4.97	0.21	129.3	0.539	69.7	116.60	117.66	11.6	0.0	0.0	1.1	-1.1	0.0
08/07/2016	6.44	0.81	5.23	0.20	129.3	0.539	69.7	117.66	118.68	10.6	0.0	0.0	1.0	-1.0	0.0
09/07/2016	6.31	0.81	5.09	0.18	129.3	0.539	69.7	118.68	119.59	9.7	0.0	0.0	0.9	-0.9	0.0
10/07/2016	5.35	0.80	4.29	0.16	129.3	0.539	69.7	119.59	120.29	9.0	0.0	0.0	0.7	-0.7	0.0
11/07/2016	6.92	0.80	5.51	0.15	129.3	0.539	69.7	120.29	121.12	8.2	0.0	0.0	0.8	-0.8	0.0
12/07/2016	8.06	0.79	6.38	0.14	129.3	0.539	69.7	121.12	122.00	7.3	0.0	0.0	0.9	-0.9	0.0
13/07/2016	6.20	0.77	4.77	0.12	129.3	0.539	69.7	122.00	113.93	15.4	8.7	0.0	0.6	8.1	0.0
14/07/2016	5.35	0.77	4.11	0.26	129.3	0.539	69.7	113.93	114.99	14.3	0.0	0.0	1.1	-1.1	0.0
15/07/2016	1.85	0.77	1.42	0.24	129.3	0.539	69.7	114.99	83.98	45.3	31.5	0.1	0.3	31.0	0.0
16/07/2016	4.74	0.75	3.56	0.76	129.3	0.539	69.7	83.98	86.59	42.7	0.1	0.0	2.7	-2.6	0.0
17/07/2016	5.64	0.75	4.23	0.72	129.3	0.539	69.7	86.59	89.62	39.7	0.0	0.0	3.0	-3.0	0.0

**Table S.14.** A period of the 2014 phenological soil water balance with the end of the phase of water stress. For explanation of the symbols, see Table S.10.

date	$ET_{0a} \cdot K_c W_s = ET_c$		$ET_c \cdot K_s = aET_c$		$TAW \cdot p = RAW$			$P_a - RO - aET_c - \Delta AW = DP$							
	ET <sub>0a</sub>	K <sub>c</sub> W <sub>s</sub>	ET <sub>c</sub>	K <sub>s</sub>	TAW	p	RAW	D <sub>r start</sub>	D <sub>r end</sub>	AW	P <sub>a</sub>	RO	aET <sub>c</sub>	ΔAW	DP
29/08/2014	4.52	0.86	3.89	0.37	129.5	0.570	73.8	108.93	110.36	19.1	0.0	0.0	1.4	-1.4	0.0
30/08/2014	4.63	0.86	3.98	0.34	129.5	0.570	73.8	110.36	111.73	17.8	0.0	0.0	1.4	-1.4	0.0
31/08/2014	4.87	0.86	4.19	0.32	129.5	0.570	73.8	111.73	113.07	16.4	0.0	0.0	1.3	-1.3	0.0
01/09/2014	1.79	0.86	1.54	0.34	129.5	0.631	81.7	113.07	65.59	63.9	52.4	4.4	0.5	47.5	0.0
02/09/2014	1.25	0.86	1.07	1.00	129.5	0.631	81.7	65.59	55.41	74.1	11.2	0.0	1.1	10.1	0.0
03/09/2014	1.04	0.86	0.90	1.00	129.5	0.631	81.7	55.41	54.41	75.1	1.9	0.0	0.9	1.0	0.0
04/09/2014	1.29	0.86	1.11	1.00	129.5	0.631	81.7	54.41	45.62	83.9	9.9	0.0	1.1	8.8	0.0
05/09/2014	2.54	0.86	2.18	1.00	129.5	0.631	81.7	45.62	47.80	81.7	0.0	0.0	2.2	-2.2	0.0
06/09/2014	3.54	0.86	3.04	1.00	129.5	0.631	81.7	47.80	50.84	78.7	0.0	0.0	3.0	-3.0	0.0

**Table S.15.** A period of the 2014 phenological soil water balance; the return of the runoff and the deep percolation. For explanation of the symbols, see Table S.10.

date	$ET_{0a} \cdot K_c W_s = ET_c$		$ET_c \cdot K_s = aET_c$		$TAW \cdot p = RAW$			$P_a - RO - aET_c - \Delta AW = DP$							
	ET <sub>0a</sub>	K <sub>c</sub> W <sub>s</sub>	ET <sub>c</sub>	K <sub>s</sub>	TAW	p	RAW	D <sub>r start</sub>	D <sub>r end</sub>	AW	P <sub>a</sub>	RO	aET <sub>c</sub>	ΔAW	DP
15/11/2014	1.39	1.04	1.44	1.00	129.5	0.681	88.2	4.89	4.08	125.4	2.2	0.0	1.4	0.8	0.0
16/11/2014	1.61	1.04	1.67	1.00	129.5	0.681	88.2	4.08	2.81	126.7	2.9	0.0	1.6	1.3	0.0
17/11/2014	0.53	1.04	0.55	1.00	129.5	0.681	88.2	2.81	(-16.43)	129.5	33.4	13.6	0.6	2.8	16.4
18/11/2014	1.75	1.04	1.81	1.00	129.5	0.681	88.2	0.00	(-1.00)	129.5	2.8	0.0	1.8	0.0	1.0
19/11/2014	0.78	1.08	0.85	1.00	129.5	0.681	88.2	0.00	(-4.34)	129.5	5.2	0.0	0.9	0.0	4.3
20/11/2014	0.47	1.08	0.51	1.00	129.5	0.681	88.2	0.00	0.32	129.2	0.2	0.0	0.5	-0.3	0.0
21/11/2014	0.53	1.08	0.57	1.00	129.5	0.681	88.2	0.32	0.83	128.7	0.1	0.0	0.6	-0.5	0.0
22/11/2014	0.43	1.08	0.47	1.00	129.5	0.681	88.2	0.83	1.27	128.2	0.0	0.0	0.5	-0.5	0.0
23/11/2014	0.45	1.08	0.48	1.00	129.5	0.681	88.2	1.27	1.59	127.9	0.2	0.0	0.5	-0.3	0.0
24/11/2014	0.38	1.08	0.41	1.00	129.5	0.681	88.2	1.59	1.78	127.7	0.2	0.0	0.4	-0.2	0.0
25/11/2014	0.40	1.08	0.43	1.00	129.5	0.681	88.2	1.78	2.15	127.3	0.1	0.0	0.4	-0.3	0.0
26/11/2014	0.42	1.08	0.45	1.00	129.5	0.681	88.2	2.15	(-2.58)	129.5	5.2	0.0	0.5	2.1	2.6
27/11/2014	0.43	1.08	0.46	1.00	129.5	0.681	88.2	0.00	(-3.41)	129.5	3.9	0.0	0.5	0.00	3.4
28/11/2014	0.40	1.08	0.43	1.00	129.5	0.681	88.2	0.00	0.25	129.3	0.2	0.0	0.4	-0.2	0.0

SUPPLEMENTARY MATERIAL 6 - MONTHLY VALUES  
OF THE PHENOLOGICAL SOIL WATER BALANCE IN  
THE PERIOD 2013-2019

For ease of reading, the values are shown at two-year intervals.

It should be noted that the phenological soil water balance (in bold in the tables) is valid at each time interval (daily, weekly, monthly, annual, multiannual). The relationships between the preliminary parameters are valid instead at daily intervals. For example for equation 7 in the text we have that:

$$ET_c = ET_{0a} \cdot K_{c\ ws}$$

However, the monthly values are sums (such as  $ET_{0a}$  and  $ET_c$ ) or weighted sums (such as  $K_{c\ ws}$ ) and therefore the equation does not work well with these values (there is a small error). But these values are derived from daily values that are correct, values for which equation 7 is perfectly valid.

**Table S.16.** Monthly values of the phenological soil water balance in the period 2013-2014.

		$ET_{0a}$	$K_{c\ ws}$	$ET_c$	$P_a - RO - aET_c - \Delta AW = DP$				
					$P_a$	RO	$aET_c$	$\Delta AW$	DP
2013	January	21,4	1,07	22,8	98,7	2,7	22,8	-3,3	76,5
	February	26,9	1,01	26,8	95,6	14,7	26,8	-0,1	54,1
	March	53,1	0,87	46,8	109,3	11,1	46,8	3,4	48,0
	April	96,0	0,68	65,0	48,1	2,5	65,0	-34,3	14,8
	May	114,5	0,95	109,5	109,6	4,3	109,5	-4,2	0,0
	June	155,3	0,98	151,8	75,9	0,9	114,7	-39,7	0,0
	July	182,2	0,84	151,9	5,7	0,0	49,6	-43,9	0,0
	August	160,2	0,80	128,5	79,2	0,0	34,1	45,1	0,0
	September	110,2	0,68	73,5	53,0	0,0	47,4	5,6	0,0
	October	52,8	0,79	41,5	87,2	4,6	41,5	41,1	0,0
	November	21,6	1,04	22,0	232,7	103,4	22,0	30,3	77,1
	December	24,7	0,79	19,2	27,3	0,1	19,2	-0,6	8,6
2014	January	26,2	0,77	21,5	66,6	9,4	21,5	0,7	35,1
	February	42,6	0,90	37,3	83,7	8,2	37,3	-4,4	42,6
	March	72,7	0,73	49,3	121,6	34,6	49,3	-4,6	42,3
	April	91,0	0,84	76,1	96,8	12,2	76,1	1,1	7,5
	May	131,5	0,99	130,9	120,6	34,8	120,7	-61,8	26,9
	June	161,4	0,98	158,1	63,2	0,1	84,4	-21,3	0,0
	July	151,9	0,80	122,2	96,4	0,0	64,9	31,5	0,0
	August	155,3	0,73	113,2	20,0	0,0	73,4	-53,4	0,0
	September	79,8	0,80	63,8	125,4	6,1	62,8	56,6	0,0
	October	56,6	0,59	33,6	88,8	10,7	33,6	44,5	0,0
	November	28,1	0,99	26,0	84,8	15,6	26,0	12,0	31,1
	December	23,1	1,06	24,5	99,5	16,4	24,5	-0,8	59,5

$ET_{0a}$ : reference evapotranspiration corrected for acclivity coefficient;

$K_{c\ ws}$ : unique 'crop' coefficient of the territory;

$ET_c$ : crop evapotranspiration of the territory;

$P_a$ : precipitation values corrected for acclivity coefficient;

RO: runoff;

$aET_c$ : actual crop evapotranspiration;

$\Delta AW$ : variation of the available water with respect to the previous day; and

DP: deep percolation.

**Table S.17.** Monthly values of the phenological soil water balance in the period 2015-2016

		ET <sub>0a</sub>	K <sub>c ws</sub>	ET <sub>c</sub>	P <sub>a</sub> - RO - aET <sub>c</sub> - ΔAW = DP				
					P <sub>a</sub>	RO	aET <sub>c</sub>	ΔAW	DP
2015	January	36,3	0,72	24,6	30,2	0,5	24,6	-0,5	5,5
	February	26,6	1,04	27,5	157,7	47,8	27,5	-0,3	82,7
	March	66,3	0,84	54,2	152,5	33,5	54,2	-10,9	75,8
	April	108,5	0,68	72,3	79,1	7,6	72,3	-8,5	7,8
	May	138,1	0,93	127,5	106,8	15,9	114,5	-23,6	0,0
	June	166,2	0,97	161,0	33,6	0,0	95,6	-62,0	0,0
	July	206,0	0,83	170,5	2,9	0,0	19,5	-16,6	0,0
	August	148,3	0,78	115,9	51,2	0,0	31,0	20,2	0,0
	September	104,1	0,69	65,3	62,9	0,0	27,9	35,0	0,0
	October	41,9	0,88	37,7	119,6	2,7	37,7	67,4	11,8
	November	30,1	0,65	19,0	52,5	5,6	19,0	-1,7	29,6
	December	14,0	0,31	4,9	1,7	0,0	4,9	-3,2	0,0
2016	January	34,1	0,89	30,0	75,6	13,6	30,0	-8,1	40,2
	February	42,7	0,84	34,6	101,9	11,8	34,6	13,7	41,8
	March	62,4	0,88	51,2	109,7	21,1	51,2	-11,1	48,4
	April	102,5	0,71	72,6	53,4	2,1	72,6	-21,3	0,0
	May	129,3	1,00	129,2	96,9	17,3	127,8	-52,2	4,0
	June	151,4	0,98	147,8	84,8	4,8	104,8	-24,8	0,0
	July	176,4	0,77	136,9	62,0	0,1	51,9	10,0	0,0
	August	153,1	0,68	104,0	11,9	0,0	33,2	-21,3	0,0
	September	96,9	0,74	70,4	55,4	0,0	34,9	20,5	0,0
	October	42,3	0,93	37,9	78,6	0,0	35,8	42,8	0,0
	November	28,4	1,06	29,9	99,6	8,0	29,9	55,0	6,7
	December	24,1	0,31	8,4	4,0	0,0	8,4	-4,5	0,0

ET<sub>0a</sub>: reference evapotranspiration corrected for acclivity coefficient;

K<sub>c ws</sub>: unique 'crop' coefficient of the territory;

ET<sub>c</sub>: crop evapotranspiration of the territory;

P<sub>a</sub>: precipitation values corrected for acclivity coefficient;

RO: runoff;

aET<sub>c</sub>: actual crop evapotranspiration;

ΔAW: variation of the available water with respect to the previous day; and

DP: deep percolation.

**Table S.18.** Monthly values of the phenological soil water balance in the period 2017-2019.

		ET <sub>0a</sub>	K <sub>c ws</sub>	ET <sub>c</sub>	P <sub>a</sub> - RO - aET <sub>c</sub> - ΔAW = DP				
					P <sub>a</sub>	RO	aET <sub>c</sub>	ΔAW	DP
2017	January	21,3	0,9	17,9	85,4	17,8	17,9	2,1	47,6
	February	38,6	0,9	33,3	82,1	13,5	33,3	1,8	33,5
	March	86,2	0,5	41,3	44,5	12,5	41,3	-24,3	14,9
	April	108,8	0,7	79,1	72,1	3,6	79,1	-10,6	0,0
	May	140,5	1,0	142,1	46,7	0,0	114,0	-67,4	0,0
	June	194,9	1,0	195,2	14,3	0,0	22,5	-8,2	0,0
	July	208,5	0,8	164,2	35,2	0,0	35,6	-0,4	0,0
	August	184,9	0,7	135,0	11,3	0,0	20,3	-9,0	0,0
	September	97,3	0,8	79,7	162,5	2,9	61,9	97,7	0,0
	October	64,3	0,5	31,0	15,4	0,0	31,0	-15,7	0,0
	November	31,3	1,0	30,5	110,4	15,6	30,5	40,9	23,5
	December	28,5	1,1	30,7	72,4	5,8	30,7	-1,6	37,4
2018	January	31,7	0,6	17,8	11,4	0,0	17,8	-8,0	1,6
	February	20,3	1,0	20,6	194,4	42,9	20,6	8,4	122,5
	March	60,7	0,9	51,0	138,4	17,6	51,0	-13,7	83,5
	April	110,4	0,7	76,5	33,1	0,1	76,5	-43,5	0,0
	May	114,8	1,0	111,0	94,9	2,6	111,0	-18,6	0,0
	June	154,4	0,9	145,4	18,0	0,0	59,9	-41,9	0,0
	July	174,1	0,8	133,1	71,0	0,0	54,6	16,5	0,0
	August	149,6	0,7	104,0	19,8	0,0	27,5	-7,7	0,0
	September	95,9	0,6	61,4	50,3	0,0	42,5	7,9	0,0
	October	48,8	0,8	39,3	76,6	0,0	37,2	39,4	0,0
	November	22,0	0,9	18,3	94,9	6,4	18,3	61,1	9,0
	December	19,9	1,0	19,6	52,5	5,1	19,6	-6,8	34,6
2019	January	24,4	1,0	24,1	68,2	2,9	24,1	6,8	34,5
	February	45,6	0,7	29,1	22,1	1,3	29,1	-19,2	10,9
	March	90,4	0,5	46,5	34,0	0,5	46,5	-12,9	0,0
	April	89,2	0,7	65,8	76,6	1,4	65,8	9,4	0,0
	May	98,0	1,0	96,4	189,1	39,6	96,4	18,5	34,6
	June	183,4	1,0	176,5	2,4	0,0	115,0	-112,6	0,0
	July	176,6	0,8	134,6	81,8	0,1	46,1	35,6	0,0
	August	155,3	0,7	106,9	29,9	0,0	63,6	-33,7	0,0
	September	103,2	0,7	74,4	79,9	0,0	51,4	28,5	0,0
	October	58,4	0,5	29,5	39,2	0,0	29,4	9,8	0,0
	November	30,1	1,0	29,9	123,7	8,8	29,9	72,4	12,6
	December	45,2	0,7	28,7	56,0	5,9	28,7	0,6	20,8

ET<sub>0a</sub>: reference evapotranspiration corrected for acclivity coefficient;

K<sub>c ws</sub>: unique 'crop' coefficient of the territory;

ET<sub>c</sub>: crop evapotranspiration of the territory;

P<sub>a</sub>: precipitation values corrected for acclivity coefficient;

RO: runoff;

aET<sub>c</sub>: actual crop evapotranspiration;

ΔAW: variation of the available water with respect to the previous day; and

DP: deep percolation.

## SUPPLEMENTARY MATERIAL 7

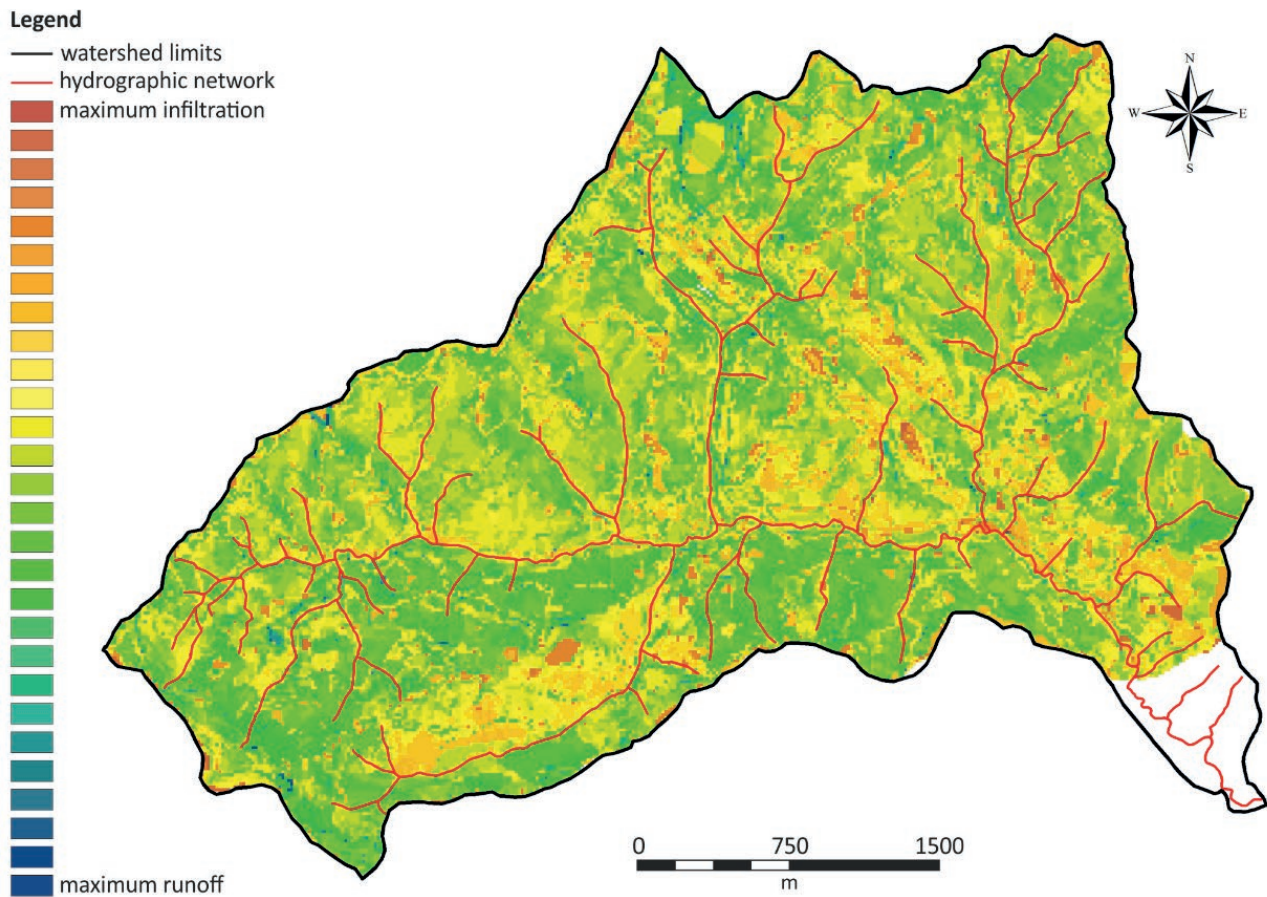


**Figure S5.** Map of the infiltration/runoff propensity obtained as overlapping layers of land use, hydrologic soil groups, slope and aspect. The processing was carried out up to the section in which the discharges of the Santa Maria degli Angeli stream were measured.